Arthropod Structure & Development xxx (xxxx) xxx

Contents lists available at ScienceDirect

Arthropod Structure & Development

journal homepage: www.elsevier.com/locate/asd

Surf and turf vision: Patterns and predictors of visual acuity in compound eye evolution

Kathryn D. Feller [a, *], Camilla R. Sharkey [b], Alyssa McDuffee-Altekruse [c], Heather D. Bracken-Grissom [d], Nathan P. Lord [e], Megan L. Porter [f], Lorian E. Schweikert [d]

[a] Union College, Department of Biological Sciences, 807 Union St., Schenectady, NY, 12308, USA
[b] University of Minnesota, Ecology Evolution and Behavior Department, Saint Paul, MN, USA
[c] University of Minnesota, Biology Teaching and Learning Department, Minneapolis MN, USA
[d] Institute of Environment, Department of Biological Sciences, Florida International University, North Miami, FL 33181, USA
[e] Louisiana State University, Entomology Department, Baton Rouge, LA, USA
[f] University of Hawai'i at Mānoa, Department of Biology, Honolulu, HI, USA

ARTICLE INFO

Article history:
Received 30 June 2020
Accepted 13 October 2020
Available online xxx

Keywords:
Arthropod phylogeny
Spatial resolution
Light
Sensory ecology
Crustacea
Hexapoda

ABSTRACT

Eyes have the flexibility to evolve to meet the ecological demands of their users. Relative to camera-type eyes, the fundamental limits of optical diffraction in arthropod compound eyes restrict the ability to resolve fine detail (visual acuity) to much lower degrees. We tested the capacity of several ecological factors to predict arthropod visual acuity, while simultaneously controlling for shared phylogenetic history. In this study, we have generated the most comprehensive review of compound eye visual acuity measurements to date, containing 385 species that span six of the major arthropod classes. An arthropod phylogeny, made custom to this database, was used to develop a phylogenetically-corrected generalized least squares (PGLS) linear model to evaluate four ecological factors predicted to underlie compound eye visual acuity: environmental light intensity, foraging strategy (predator vs. non-predator), horizontal structure of the visual scene, and environmental medium (air vs. water). To account for optical constraints on acuity related to animal size, body length was also included, but this did not show a significant effect in any of our models. Rather, the PGLS analysis revealed that the strongest predictors of compound eye acuity are described by a combination of environmental medium, foraging strategy, and environmental light intensity.

1. Introduction

Vision is a key sensory modality for the survival of many organisms as they navigate life in a given environment. Different visual information can be parsed from the multiple dimensions of light, which can be described by intensity, wavelength (perceived as color), e-vector orientation (polarization), and directionality. Different combinations of intensity (Warrant et al., 1996), wavelength (Osorio and Vorobyev, 1996), and polarization information (Sharkey et al., 2015) are used to enhance the contrast of a visual scene, whereas directional light information gathered by an eye is fundamental for assembling a perceived image of the external world. The term *visual acuity* is used to define how spatial details of this directional information are resolved by an eye, which can be referred to by its empirical metric *cycles per degree* (CPD; Caves et al., 2018). Visual acuity impacts multiple aspects of an animal's ecology, including reproduction, navigation, feeding, predation, and escape (Warrant and McIntyre, 1993). Consideration of visual acuity and the selective pressures that impact acuity are important for studies that seek to link ecology and evolution of animal vision (Land, 1997; Caves et al., 2018).

The highest visual acuities achieved in nature are by animals who possess camera-type eyes with a single, large lens positioned over an array of photoreceptors. By comparison, compound eyes are a composite of multiple optical units, or ommatidia, each with its own tiny lens. Relative to the camera eyes of humans and most vertebrates, compound eye visual acuity is terrible. The highest compound eye acuity measured is 100 x lower than the average human visual system and 10 x lower than the cut-off for human legal blindness (Caves et al., 2018). The angular resolution of the compound eye-type is ultimately limited to much lower levels by diffraction from the small lenses in each ommatidium (Kirschfeld,

* Corresponding author.
E-mail address: fellerk@union.edu (K.D. Feller).

https://doi.org/10.1016/j.asd.2020.101002

1976). Compound eye acuity can be optically improved by increasing the number of facets (i.e. lenses) or the facet diameter (aperture) of each lens, though both solutions come with the cost of generating greater surface area. Generally, larger compound eyes yield more acute vision, though these larger eyes must in turn be supported by a larger animal (Kirschfeld, 1976). We see this play out in allometric studies of organisms such as bees (Jander and Jander, 2002), damselflies (Scales and Butler, 2016), and butterflies (Rutowski et al., 2009), where a positive correlation exists between compound eye acuity and body size. We expect, given these previous studies, that a similar correlation between body size and acuity persists across all arthropod lineages, whereby larger animals have greater visual acuities.

In the context of compound eye evolution, however, body size is just one of several ecological factors that may influence visual acuity. As visual systems evolve to meet the needs of their users, the first major factor to consider in shaping the visual acuity is an animal's behavior. Because compound eyes are composites of multiple ommatidial units, the topography of acuity may vary across an eye to suit different behaviors (Smolka and Hemmi, 2009). A small region of high visual acuity, called an acute zone, may be suited for a specific, sometimes singular, behavioral task. An acute zone often, but not necessarily, contains facets with larger diameters (apertures) and minimized angles between each photoreceptor (interommatidial angle). The acceptance angle, or region of view, for ommatidia in an acute zone may also be minimized using various optical features such as: focal length, or distance between the base of the light focusing system and the point at which rays of incident light are brought into focus; refractive index, the speed at which light travels through a medium, which underlies how much incident rays are refracted; and/or internal aperture controls from mechanisms such as pigment migration (for review see Warrant and McIntyre, 1993). Different combinations of these strategies are exemplified in predators that pursue small, fast moving targets, including dragonflies (Land, 1997), robber flies (Wardill et al., 2017), and killer flies (Gonzalez-Bellido et al., 2011). The visual demands required for stabilizing such targets on the retina, while the predator gives chase, have led to the evolution of some of the best acuity measures recorded from compound eyes. Thus, we hypothesize that animals evolved to hunt small, moving targets will have higher visual acuities than those that neither pursue nor ambush targets, regardless of the alternate foraging strategy.

Arthropods occupy almost every habitable place on Earth, resulting in visual requirements that vary with environment (Warrant and McIntyre, 1993). The second ecological factor understood to impact compound eye visual acuity is the habitat-specific environmental light level, or intensity (Caves et al., 2016). The environmental light intensity is closely associated with the fundamental trade-off between the visual acuity (or resolution) and light sensitivity of an eye. For example, to improve vision in dim light, nocturnally active species will often improve their probability for photon capture (increase their sensitivity) by widening the aperture of the facets, which, if the animal cannot support a larger eye, results in a reduction in the number of ommatidia, ultimately decreasing visual acuity (Warrant, 2008). This trade-off between light sensitivity and resolution may also be driven by microhabitat, or areas within a larger habitat that vary in light levels, as is seen in damselflies (Scales and Butler, 2016) and psyllids (Farnier et al., 2015). Apposition and superposition optical eye types are generally associated with selection towards increased resolution or sensitivity, respectively. In the apposition eye, light from a single lens is focused onto the photoreceptive unit below, maximizing the resolution of a detected image. In the superposition eye however, light is pooled from multiple lenses onto a single photoreceptive unit, resulting in an increase in sensitivity. While it is often assumed that this gain in sensitivity is at the expense of resolution, some insects with superposition eyes are able to preserve spatial acuity at different light intensities via flexible spatial filtering at the neural level (Stöckl et al., 2020).

A third ecological factor linked to visual acuity is the complexity of space in a visual scene. Though the complexity of a visual scene has been linked to acuity in ray-finned fishes (Caves et al., 2017), this factor is less understood for animals with compound eyes. Recent advances in the methods used to characterize the light field of a spatial scene describe a band of spatial information around the horizon of the majority of imaged scenes, with the exception of scenes where the sky is blocked from view, such as a dense tropical rainforest (Warrant et al., 2020; Nilsson and Smolka, submitted). A relationship between horizontal structure of a visual scene and visual acuity is known in fiddler crabs, which have elongated acute zones that are exceptional for picking out threats above the horizon (Zeil and Hemmi, 2005). We hypothesize that since compound eye acuity is often too poor to resolve spatial details in a complex scene, that the presence of a horizon in the environmental light field will correlate more strongly with the acuity of a compound eye.

Both environmental intensity and structure of the light field lead to differences in the sighting distance of an object, or how far away something can be detected. Objects are more difficult to spot in dim light or when they blend into the background. Additionally, dramatic differences in sighting distance exist between terrestrial (air) and aquatic (water) habitats, simply from the difference in the physical interaction of light with the two media (Ruxton and Johnsen, 2016). Even with the highest possible visual acuity, absorption and scatter of light underwater drastically decreases the distance at which one can view an object. For example, a flock of birds is more easily spotted from 100 m away than a school of fish at the same distance, subtending the same visual angle (Ruxton and Johnsen, 2016). With increased viewing distance, an object becomes indistinguishable from the background due to the loss of the object's radiance to absorption and scatter as well as the number of photons scattered into the visual path from the surrounding environment (Cronin et al., 2014). This degradation of visual contrast underwater cannot be overcome by improving the visual acuity of any eye, whether camera or compound. To this end, we hypothesize that evolution in a water medium, being highly light-scattering and viscous, favors sensory modalities that, unlike acute vision, are less distance-dependent and better transduced through water, such as mechanosensation (Budelmann, 1989) or chemosensation (Nowińska and Brozek, 2020). In consideration of this fourth ecological factor (environmental medium), we predict that animals evolved to live in water will have lower visual acuities than animals living in air. Further, diffraction-limited compound eyes provide an excellent system to test this hypothesis due to the extreme evolutionary diversity and range of habitats occupied by Arthropoda. Relative to camera-type eyes, the range of compound eye visual acuities is much narrower and at lower degrees of resolvability. Selection for increased acuity in terrestrial vs. aquatic systems may, therefore, be more pronounced in compound eyes than other eye types.

Considering these four major ecological factors that may impact compound eye visual acuity, we predict that the highest acuities occur in animals that are large predators of small prey residing in bright, terrestrial (air) habitats dominated by a strong horizon. The fact that so many ecological factors are expected to impact compound eye acuity raises the question: in what combination(s) do these factors work together to determine the maximum acuity of a compound eye? Since organisms and their traits evolve as integrated wholes, we expect multiple ecological pressures to shape the evolution of visual acuity in concert with one another, rather than in isolation (Gould and Lewontin, 1979). In this paper, we set

out to address how multiple factors (body size, environmental light levels, foraging strategy, environmental medium, and horizontal structure of the visual scene) act on the evolution of compound eye visual acuity in the arthropod lineage, while accounting for the effects of shared evolutionary history. Few studies have attempted to examine these relationships across diverse taxa, either in vertebrates (Veilleux and Kirk, 2014; Caves et al., 2017) or invertebrates (Cronin, 1986; Land, 1997; Caves et al., 2018). With the exception of these cross-taxa studies, most research on the evolution of acuity has focused on selection from a single trait or ecological factor. We used a phylogenetic generalized least squares (PGLS) modelling approach to examine multiple ecological factors and how they predict acuity in diverse arthropod lineages (Freckleton et al., 2002; Adams, 2008), a method that has been applied in similar studies of vision in camera-type eyes (Caves et al., 2017; Schweikert et al., 2018). In addition to providing a comprehensive survey of compound eye visual acuities, this study reveals some of the key patterns and predictors that shape the evolution of visual acuity in compound eyes.

2. Methods

2.1. Visual acuity database construction

Data were compiled from the literature to build a database of visual acuity metrics for compound eyes. We used an established metric for visual acuity, cycles per degree (CPD), to make comparisons across diverse evolutionary lineages (as in Caves et al., 2018). CPD was determined for each species in the database using one of three methods. First, if a publication reported discrete CPD measurements from either behavioral or optical studies, we recorded the maximum CPD for a given species. Since such studies were few (9/109 database references; Table S2), our second method used the following formula to estimate CPD:

$$CPD = \frac{1}{\Delta\rho} \quad (1)$$

where $\Delta\rho$ is the minimum reported acceptance angle, or half-width of the angular sensitivity functions (as in Caves et al., 2018). In the absence of $\Delta\rho$, CPD was estimated by a third method:

$$CPD = \frac{1}{2\Delta\phi} \quad (2)$$

where $\Delta\phi$, is the minimal interommatidial angle, or angle of separation between photoreceptors, reported from the eye of a given species in a single study. Though the minimum reported value was taken for each value of $\Delta\phi$ and $\Delta\rho$, a hierarchical rule of logic was used for determining the best estimate of CPD from these parameters. Since $\Delta\rho$ represents multiple optical parameters, a reported $\Delta\rho$ was always used to determine CPD, regardless of $\Delta\phi$. This includes situations where a visual system was reported to oversample visual space ($\Delta\rho > 2\Delta\phi$), such as the elephant hawkmoth (*Deilephila elpenor*), the carpenter bee (*Xylocopa tranquebarica*), or the toebiter (*Lethocerus insulanus*). All remaining calculations were derived from $\Delta\phi$. We acknowledge that calculations of CPD from $\Delta\phi$ may overestimate acuity for eyes that pool spatial information, however, these methods provide the best-case estimation for the visual system of a given species in the absence of discrete $\Delta\rho$ recordings.

To demonstrate the variation found in arthropod visual acuity, we modeled how representative species of the maximum, minimum, and median visual acuity values in our database may view a given scene using the *AcuityView* package (v 0.1; Caves and Johnsen, 2018) in R (v. 3.4.4; R Core Team, 2018). Using estimates of acuity, *AcuityView* portrays how a scene might be perceived by removing information that would not be detectable to animals given their spatial resolution. We used the mean body length of all species in the database to generate a series of ecologically relevant viewing distances to visually assess the performance of each CPD value. Three viewing distances were then calculated by multiplying mean body length by a factor of one, ten, and one hundred. The *AcuityView* outputs were then visually assessed and compared in the context of three species that represent the max, min and average visual acuity values. Note, *AcuityView* does not account for changes in field of view that occur with distance. Rather, it renders an image to portray changes in spatial information available to a given viewer.

2.2. Assignment of ecological variables

Six independent variables were scored for each species in the database: eye type, body length, environmental medium, environmental light intensity, foraging strategy, and horizontal structure of the visual scene. Eye type was scored as *apposition*, *superposition*, or *neural superposition* only for species specifically reported as such. In the apposition eye type, each ommatidium samples an individual point in space, whereas superposition eyes pool spatial information from multiple points onto a single photoreceptor. Our superposition score included all reported optical variations of spatial summation, such as reflecting, refracting, parabolic, and proximal lens types. Neural superposition eyes were treated as a third category since these eyes represent an intermediary eye type defined by possession of apposition optics with spatial summation at the level of the photoreceptors or nervous system. For species whose eye types have yet to be characterized, this parameter was left blank, creating an unequal sample size relative to scoring of the ecological factors.

Though eye size is more strongly associated with increased acuity in camera type eyes (Caves et al., 2018), arthropod compound eye size is poorly described and understudied by comparison (Gaspar et al., 2020). Therefore, since there is an established precedent that compound eye acuity increases with body size (Jander and Jander, 2002; Rutowski et al., 2009; Scales and Butler, 2016), we included this factor in our analyses in place of eye size. Body size was defined as the longest axis of the body, or body length. In the majority of cases, body length was measured as the distance from the most anterior/rostral point of the head to the most posterior/caudal point of the abdomen. Most crab species, however, presented an exception. Since crab bodies are wider than they are long, crab body length was reported as the width of the carapace. Body lengths reported alongside a specific acuity measure were taken as priority metrics; however, few studies reported the body lengths of the individuals measured. For the remaining species, mean adult body lengths were estimated from reports in the literature and online naturalist resources, or, in the absence of a reported value, were measured from calibrated images in ImageJ (Fiji/ImageJ; Schindelin et al., 2012). To test for a linear relationship between body length and visual acuity, both body length and CPD values were log transformed, plotted against one another, and fit to a linear model using the *lm* function in R v. 3.4.3 (www.r-project.org).

Environmental medium was defined as the physical medium through which an organism primarily views the world. Medium was scored as *air, water,* or *both* (for animals with amphibious behavior). In both air and water media, animals experience ranges of light intensities that vary over many orders of magnitude depending on both the environment they occupy and their

behavioral ecology. For the majority of species in our database, the specific behavioral patterns and environmental irradiances have yet to be quantified. Due to these limitations, we adopted a set of broad criteria to score the environmental light intensity of each species as either *bright* or *dim*. *A dim* environmental light intensity score was given to species if they fulfilled one of the following critera: occur at depths greater than 100 m, perform nocturnal or crepuscular vertical migrations to the surface, or display nocturnal or crepuscular patterns of activity in the *absence* of daytime activity. If quantified illumination ranges were available for each species, we identified that the cutoff between *dim* and *bright* light environments would be approximately 1 lux. Underwater, total surface irradiance is attenuated by up to 99% at 100 m depth for most Jerlov categories of water, with daytime illumination levels occurring below 1 lux at greater depths (Jerlov, 1977). In air, illumination also falls below 1 lux for nocturnal moonlight (Johnsen, 2012). Aquatic species were scored as *bright* if they occupied depths shallower than 100 m. In a few cases, the reported depth range straddled 100 m. In such situations the species was only classified as *bright* if their daytime range reached within 1 m of the surface, since this would result in exposure to 50% of surface quanta for all water types (Jerlov, 1977). Animals that live in air were categorized as *bright* if they were reported as diurnal. In a few cases where a species is reported as equally active during both day and night, these species were scored as *bright* since they were exposed to large photon quanta for part of their active cycle. Though the *bright* light environment criteria of >1 lux encompasses a much greater range of values (up to 10^5 lux), such assignment criteria allowed us to look for trends in visual acuity in environments that present many photons versus very few photons.

To examine how acuity varies with the structure of spatial information in visual scene ('visual scene structure'), the habitat in which a species primarily occurs was scored as either horizon present or absent. New methods on the environmental light fields of diverse visual scenes reveal that horizon structure of light information is present in most habitats and with changing light levels (Warrant et al., 2020). Two main habitats are devoid of this horizontal radiance information: rainforests (Nilsson and Smolka, submitted) and the pelagic environment (Johnsen, 2002; Caves et al., 2017). Species that occur in either of these two habitats were thus scored as having no horizon (*none*) in the visual scene structure, whereas all other species received a *horizon* score (including benthic species).

The established link between visual acuity and predatory foraging strategies underpinned our decision to include this behavioral score in our meta-analysis (Land and Nilsson, 2002). Predation was defined as the acquisition of motile prey, which can be described by two main strategies: *ambush* predation, where the predator sits and waits to make a calculated strike, and *pursuit* predation, where the predator localizes, pursues, and captures a moving target. All other foraging strategies were categorized as *other*. Since we were interested in testing the association between active visual predatory behavior and visual acuity, the *other* category was very diverse, including scavengers, detritivores, herbivores, omnivores, opportunistic or non-specialized predators, parasites, symbiotes as well as predators of non-motile prey. For species with generalist diets, an animal was categorized as *other* when motile prey constituted less than half of their diet as determined by gut content studies.

2.3. Phylogenetic tree reconstruction

To perform a PGLS analysis, we required a phylogeny with a 1:1 relationship between taxa with visual acuity data and those in the species tree. As no such phylogeny exists, we aimed to generate a phylogeny that adhered as closely as possible to currently accepted relationships, according to extensive genomic and transcriptomic studies (Lozano-Fernandez et al., 2019). There were limited shared loci available for our desired taxa, particularly for crustaceans. Thus, to stabilise deep nodes, we used a protein supermatrix of 272 genes (von Reumont et al., 2012), in combination with DNA loci, to generate the required phylogenetic breadth that is lacking in the latest Pancrustacean-omics studies (Lozano-Fernandez et al., 2019).

The original 92 taxon supermatrix ($2A_{red}$) was trimmed of all seven polyneopteran species (*Laupala kohalensis, Gryllus bimaculatus, Locusta migratoria, Blattella germanica, Reticulitermes flavipes, Hodotermopsis sjoestedti, Periplaneta americana*) to account for the incorrect placement of Hemiptera as a sister group to Polyneoptera, in the original analysis from von Reumont et al. (2012). All available DNA sequences from three mitochondrial loci (COI, 12 S, 16 S) and two nuclear loci (18 S and H3) for our target taxa and 83 taxa in the protein supermatrix were downloaded from GenBank. These five genes were chosen due to their phylogenetic utility in previous studies of Pancrustacea (Bybee et al., 2011) and the availability of mitochondrial genomes for many taxa, yielding full-length COI, 12 S and 16 S sequences (see Table S1 for loci information per species). Additionally, three previously unpublished sequences (16 S, 18 S and H3) from *Dioptromysis spinosa* were included (for methods see Porter, 2005). For species where there were few loci available and phylogenetic placement or support was poor, available loci were pooled across multiple species to generate a new chimeric taxon to represent the genus.

DNA sequences were aligned with MAFFT v. 7.453 (Katoh et al., 2002; Katoh and Standley, 2013) using automatic alignment strategy detection and allowing for reverse complementing of sequences. Sequences were lightly trimmed with trimAl v. 1.2 (Capella-Gutiérrez et al., 2009) to remove gaps present in >95% of sequences and poorly aligned sequences were removed. Sequences were then concatenated using SequenceMatrix v1.8 (Vaidya et al., 2011). Trees were inferred from a partitioned data matrix of five DNA loci and one protein supermatrix from 418 species with the GTR + I + G DNA model (Abadi et al., 2019) and the LG + I + G4 protein models selected, respectively, according to preliminary testing with ModelFinder (Kalyaanamoorthy et al., 2017). Partitions were assigned as follows: 12 S: 1–1086; 16 S: 1087–2774; 18 S: 2775–5217; COI: 5218–6762; and protein supermatrix: 1–54209. All compiled gene data text files and alignments were deposited into a public database (Dryad; https://doi.org/10.5061/dryad.3n5tb2rdr).

The phylogeny was inferred using maximum likelihood (IQ-TREE v. 1.6.12; Nguyen et al., 2015) with 1000 UFBoot iterations (Hoang et al., 2018), the SH-like approximate likelihood ratio test (aLRT) with 1000 bootstrap replicates and a Bayesian-like transformation of aLRT (aBayes) test (Anisimova et al., 2011). Tree searches were repeated 10 times and the phylogeny that most accurately resolved currently accepted relationships was used for further analysis by comparison with studies that used more extensive gene sampling (Misof et al., 2014; Schwentner et al., 2017; Lozano-Fernandez et al., 2019). Trees were visualised using FigTree v. 1.4.4 (http://tree.bio.ed.ac.uk/software/figtree/) and edited in Adobe Illustrator (CS6).

Since sequence data used to construct the phylogeny were not available for all represented species in the compound eye acuity database, only a subset of the reported data in the database could be used to conduct phylogenetically-corrected meta-analyses. These data are referred to as the *phylogeny subset*. The degree of phylogenetic signal in acuity was estimated within the phylogeny subset by calculating Pagel's lambda (λ; Pagel, 1999; Freckleton

et al., 2002) using the *phytools* v. 0.6 package (Revell, 2011) in R v. 3.4.3 (www.r-project.org). Pagel's λ is a branch length transformation that maximizes the likelihood of the observed data. λ can range from 0 (phylogenetic independence) to 1 (direct covariance with phylogenetic structure). A likelihood ratio test was used to determine significance against the null hypothesis that $\lambda = 0$.

2.4. Phylogenetic generalized least squares models and statistical analyses

We found significant phylogenetic signal in visual acuity (Pagel's $\lambda = 0.8122$; $p < 0.001$) indicating that it is necessary to account for shared phylogenetic history in our analysis. A phylogenetically-corrected linear model was used to test the relationship between compound eye acuity (CPD) and various ecological factors in R (*phylolm*; Tung Ho and Ané, 2014). This method treats visual acuity as the response variable for all possible linear combinations of parameters scored for $\log_{10}$ body length, environmental medium, environmental light intensity, foraging strategy, and visual scene structure. Eye type factor was excluded from the PGLS due to unequal sample size for this variable. In the phylogeny subset data, we included compound eye acuity data for different life stages of two dragonfly species, *Aeshna palmata* and *Anax junius*, which were each represented as duplicate branches in our molecular phylogeny. Since the larval stages of some species possess complex compound eyes that evolve to perform in a different habitat than the adult stage, these values do not represent pseudoreplication of a single node but an evaluation of ecological pressures and CPD between individuals with a genetic distance of zero, or no adjustment. Larval acuity data were not available for any other species.

A total of 32 models were tested in our PGLS analysis, representing all possible combinations of the five ecological factors tested (body length, environmental medium, environmental light intensity, foraging strategy, and horizontal structure of environmental light field), including a null model of no factors. Akaike's information criterion (*AIC*; Burnham and Anderson, 2002) was used to evaluate and rank the fit of each PGLS model output, with the lowest AIC value corresponding to the best-fit model. *ΔAIC* was calculated as the difference between the *AIC* value of a given model and the lowest *AIC* value. The best-fit model was defined as the model with the lowest *ΔAIC*, though models were accepted as showing support if *ΔAIC* was less than 4 (Burnham et al., 2011). The probability of each model (i) being the best of a given set, or model weights (w), was calculated using the formula (Burnham and Anderson, 2002):

$$w_i = \left(e^{-0.5\Delta AICi}\right)\left(\sum_i e^{-0.5\Delta AICi}\right)^{-1} \quad (3)$$

To examine the relationships within each factor considered in the best-fit model, pairwise comparisons of each factor category were carried out. Since CPD data in the phylogeny subset did not meet assumptions of normal distribution (Sharpio-Wilks test, $p < 0.05$), a non-parametric Kruskall–Wallace test was used to compare CPD for all ecological bins except environmental light intensity and visual scene structure, which were compared using a Wilcoxon rank sum test. Where appropriate, post hoc Dunn tests were used to conduct pairwise comparisons. Bonferroni correction was used to adjust the critical α-level for multiple tests. All codes used for statistical analyses and modeling were deposited in a public database (Dryad; https://doi.org/10.5061/dryad.3n5tb2rdr).

3. Results

3.1. Pancrustacean phylogeny

Our full phylogeny of 418 taxa broadly recovered well-accepted relationships across Pancrustacea (Fig. S1) according to more taxon-specific phylogenies constructed in previous work (Lozano-Fernandez et al., 2019). Most major nodes were congruent across the ten repeated phylogenies with the exception of Neuropterida (mantispids, owlflies and relatives), which was only recovered as the sister group to Coleoptera (currently accepted hypothesis) in half of the resultant phylogenies. In addition to removing species not present in the database, four species with inconsistent placement with low support (e.g., rogue taxa) or that generated familial polyphyly were removed prior to further analyses (*Tripteroideas bambusa*, *Tipula abdominalis*, *Musca domestica* and *Cherax destructor*) (Fig. S1).

The phylogenetic relationships across Pancrustacea were well resolved by the trimmed 278 species phylogeny (Fig. 1, Fig. S2). Within Hexapoda, ordinal relationships were well resolved and consistent with the recently published, extensive phylogenies using -omics data (Misof et al., 2014; Schwentner et al., 2017; Lozano-Fernandez et al., 2019) and in most cases, species formed monophyletic family-group relationships. Two inconsistencies in familial relationships were recovered but retained for subsequent analysis. Firstly, Carabidae (*Cicindela hybrida, Asaphidion flavipes, Elaphrus riparius* and *Notiophilus* sp.) was recovered as non-monophletic but all species were correctly assigned to the subordinal level Adephaga. Secondly, within Lepidoptera, Nymphalidae was non-monophyletic, with two species (*Parantica aglea* and *Euploea mulciber*) forming a separate clade, sister to Lycaenidae. However, both Nymphalidae and Lycaenidae were correctly placed within other members of the same superfamily (Papilionoidea; Kawahara et al., 2019).

Across Crustacea, most orders and families were resolved as monophyletic and the deeper relationships (Class level) were consistent with current phylogenies (Schwentner et al., 2017; Lozano-Fernandez et al., 2019). Within the decapod crustacean family, Palaemonidae, a number of genera were recovered as polyphyletic: *Periclimenes, Cuapetes*, *Ancylomenes*. However, this is in agreement with previous findings where a similar complement of DNA loci (COI, 16 S, 18 S and H3) were used for tree inference (Horká et al., 2016). Across Stomatopoda, our results support the polyphyly of Gonodactyloidea, as has been recovered in two phylogenetic studies (Porter et al., 2010; Van Der Wal et al., 2017). However, both studies also recovered *Hemisquilla* as basal to all stomatopods, which we recovered in only one of ten phylogenies. This phylogeny was not used for further analysis, due to the poor placement of the insect clade Neuropterida. In both cases of Palaemonidae and Stomatopoda, more extensive gene sampling will be required to more conclusively resolve these intergeneric and familial relationships for future studies.

3.2. Compound eye acuity database & phylogenetic subset

From the literature, we built a compound eye visual acuity database that contains data for 385 unique arthropod species (400 total entries). These species represent six major extant arthropod classes: Hexapoda (53.5%); Malacostraca (45%); Ostracoda, Ichtyostraca, Branchiopoda, and Merostomata (together 1.5%; Table 1; Table S3). The mean acuity of all arthropod compound eyes reported in the database is 0.39 CPD (s.d. ± 0.44). These acuity values range from 0.02 CPD (springtail, *Dicyrtomina ornata* and parasitoid wasp, *Megaphragma mymaripenne*, for example) to 3.70 CPD (robberfly, *Holcocephala* sp). Underwater, the greatest compound eye

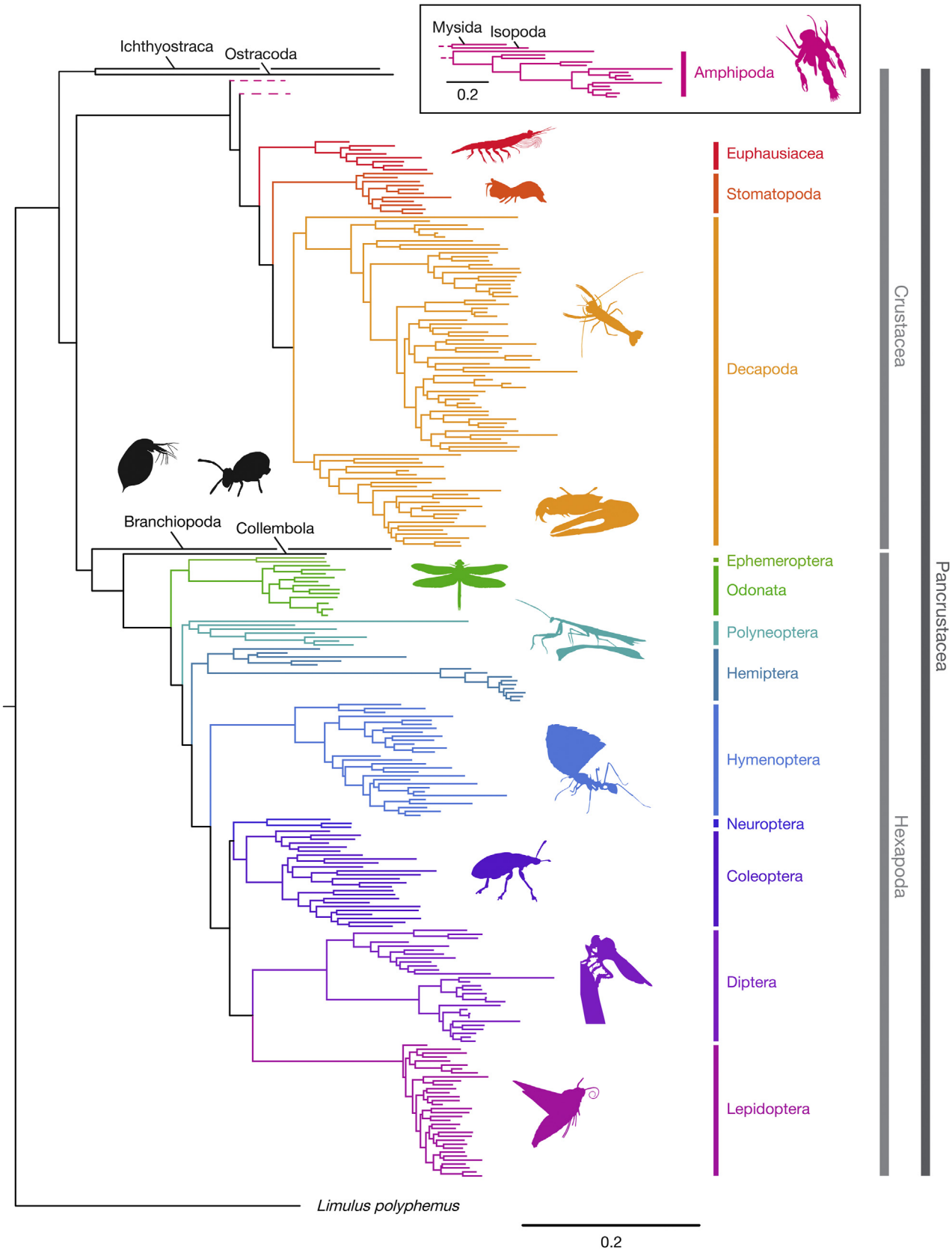

Fig. 1. Phylogeny of 278 arthropod species used for PGLS analysis. This tree is a trimmed version of a larger 418 maximum likelihood phylogeny (Fig. S1). Dermaptera, Orthoptera, Mantodea and Phasmoidea are referred to here collectively as Polyneoptera. Two species (*Aeshna juncea* and *Anax junius*) were repeated in the phylogeny (not shown). For support values and taxon labels see Fig. S2.

Table 1
Database of compound eye visual acuity data. All interommatidial angle values provided are reported from the literature (Table S2). **Bold** values for acceptance angle and CPD are reported from the literature, otherwise value provided is calculated.

Class	*Order/Family*	*Species*	*Eye Type*	*BL* (cm)	$\Delta\phi$ (deg)	$\Delta\rho$ (deg)	CPD	*Ref.*	*Common Name*
Branchiopoda	**Onychopoda**								
	Polyphemidae	*Polyphemus pediculus*	apposition	0.80	2.00	4.00	0.25	72	water-flea
Hexapoda	**Blattodea**								
	Blattidae	*Periplaneta americana*	apposition	4.00		**2.30**	0.43	12	cockroach
	Coleoptera								
	Cantharidae	*Cantharis livida*	apposition	1.25	1.80	3.60	0.28	48	soldier beetle
	Carabidae	*Asaphidion flavipes*	apposition	0.45	2.00	4.00	0.25	7	
	Carabidae	*Cicindela hybrida*	apposition	1.40	1.50	3.00	0.33	48	northern dune tiger beetle
	Carabidae	*Elaphrus riparius*	apposition	0.70	2.00	4.00	0.25	7	
	Carabidae	*Notiophilus biguttatus*	apposition	0.54	2.20	4.40	0.23	6	
	Cerambycidae	*Monochamus alternatus*	apposition	2.00	5.34	**2.42**	0.41	100	japanese pine sawyer beetle
	Chrysomelidae	*Chrysomela fastuosa*	apposition	0.60	5.40	10.80	0.09	48	dead nettle leaf beetle
	Coccinellidae	*Coccinella septempunctata*	apposition	0.75	2.90	5.80	0.17	48	seven spot ladybird
	Curculionidae	*Chlorophanus viridis*	apposition	0.64	7.00	14.00	0.07	48	
	Curculionidae	*Hypothenemus hampei*		0.12	13.60	27.20	0.04	98	coffee berry borer
	Curculionidae	*Lixus blakeae*	apposition	1.00	6.00	12.00	0.08	48	weevil
	Curculionidae	*Phyllobius urticae*	apposition	0.80	7.00	14.00	0.07	48	short nosed weevil
	Curculionidae	*Rhynchophorus ferrugineus*		3.00	1.50	3.00	0.33	39	red palm weevil
	Dytiscidae	*Dytiscus marginalis*		3.10		**40.00**	0.03	38	water beetle
	Elateridae	*Agrypnus binodulus*	superposition	2.65	1.68	3.36	0.30	68	click beetle
	Elateridae	*Melanotus cete*	superposition	1.70	1.20	2.40	0.42	68	click beetle
	Elateridae	*Melanotus legatus*	superposition	2.10	1.30	2.60	0.38	68	click beetle
	Gyrinidae	*Macrogyrus striolatus*	superposition	1.60		**2.80**	0.36	37	water beetle
	Lampyridae	*Photuris versicolor*	superposition	3.50	1.80	3.60	0.28	48	firefly
	Tenebrionidae	*Tenebrio molitor*	apposition	1.50	6.50	13.00	0.08	48	mealworm beelte
	Scarabaeidae	*Anoplognathus pallidicollis*	superposition	2.00	1.50	**3.00**	0.33	48	Christmas beetle
	Scarabaeidae	*Onitis alexis*	superposition	18.50	2.50	**4.30**	0.23	48	bronze dung beetle
	Scarabaeidae	*Sericesthis geminata*		0.90	1.50	3.00	0.33	61	
	Staphylinidae	*Creophilus erythrocephalus*	apposition	2.00		**5.13**	0.19	60	rove beetle
	Tenebrionidae	*Amarygmus morio*		2.50	5.90	11.80	0.08	48	darkling beetle
	Collembola								
	Dicyrtomidae	*Dicyrtomina ornata*	apposition	1.45	25.00	50.00	0.02	48	springtail
	Dermaptera								
	Forficulidae	*Forficula auricularia*	apposition	1.35	7.20	14.40	0.07	48	european earwig
	Diptera								
	Asilidae	*Holcocephala* sp.	NS	0.50	0.28	**0.27**	3.70	99	robber fly
	Bibionidae	*Bibio marci*	NS	1.20	1.60	**2.00**	0.50	104	hawthorn fly
	Bibionidae	*Dilophus febrilis*		0.58	2.00	**2.00**	0.50	104	
	Calliphoridae	*Calliphora erythrocephala*	NS	1.50	1.10	**1.02**	0.98	48	blow fly
	Cecidomyiidae	*Trisopsis* or *Lestodiplosis* sp.	apposition	0.25	6.00	12.00	0.083	65	midge
	Culicidae	*Aedes aegypti*	apposition	0.46	6.20	12.40	0.08	44	mosquito
	Culicidae	*Aedes albopictus*	apposition	0.63	5.10	10.20	0.10	44	mosquito
	Culicidae	*Aedes japonicus*	apposition	0.71	4.50	9.00	0.11	44	mosquito
	Culicidae	*Aedes taeniorhynchus*	apposition	0.63	4.80	9.60	0.10	44	mosquito
	Culicidae	*Anopheles albimanus*	apposition	0.44	6.20	12.40	0.08	44	mosquito
	Culicidae	*Anopheles balabacensis*	apposition	0.30	6.80	13.60	0.07	44	mosquito
	Culicidae	*Anopheles dirus*	apposition	0.42	6.70	13.40	0.07	44	mosquito
	Culicidae	*Anopheles gambiae*	apposition	0.45	6.00	12.00	0.08	44	mosquito
	Culicidae	*Anopheles minimus*	apposition	0.39	7.50	15.00	0.07	44	mosquito
	Culicidae	*Anopheles saperoi*	apposition	0.45	3.60	7.20	0.14	44	mosquito
	Culicidae	*Anopheles stephensi*	apposition	0.29	7.30	14.60	0.07	44	mosquito
	Culicidae	*Armigeres subalbatus*	apposition	0.66	5.80	11.60	0.09	44	mosquito
	Culicidae	*Culex pipiens molestus*	apposition	0.68	4.00	8.00	0.13	44	mosquito
	Culicidae	*Culex pipiens pipiens*	apposition	0.72	5.90	11.80	0.08	44	mosquito
	Culicidae	*Culex quinquefasciatus*	apposition	0.65	6.10	12.20	0.08	44	mosquito
	Culicidae	*Culex tritaeniorhynchus*	apposition	0.39	4.60	9.20	0.11	44	mosquito
	Culicidae	*Ochlerotatus togoi*	apposition	0.92	6.10	12.20	0.08	44	mosquito
	Culicidae	*Toxorhynchites brevipalpis*	apposition	1.80	2.60	5.20	0.19	44	mosquito
	Culicidae	*Tripteroides bambusa*	apposition	0.80	0.72	1.44	0.69	44	mosquito
	Drosophilidae	*Drosophila melanogaster*	NS	0.35	3.20	**8.23**	0.12	31	fruitfly
	Drosophilidae	*Drosophila melanogaster*	NS	0.30	5.00	10.00	0.10	48	fruitfly
	Empididae	*Rhamphomyia tephraea*		0.50	0.50	1.00	1.00	49	
	Glossinidae	*Glossina* sp.		1.00		**1.60**	0.63	49	tsetse fly
	Keroplatidae	*Arachnocampa luminosa*	apposition	3.50	5.50	11.00	0.09	62	
	Keroplatidae	*Neoditomyia farri*			4.00	8.00	0.13	62	
	Muscidae	*Coenosia attenuata*	NS	0.35	2.20	**2.59**	0.39	31	killer fly
	Muscidae	*Musca domestica*	NS	0.65	2.50	5.00	0.20	48	housefly
	Muscidae	*Musca domestica*	NS	0.64	1.60	3.20	0.31	50	housefly
	Psychodidae	*Telmatoscopus albipunctata*	apposition	0.25	11.00	22.00	0.05	43	moth midge
	Simuliidae	*Simulium* sp.		0.50	1.60	3.20	0.31	49	black fly
	Syrphidae	*Eristalis tenax*	NS	1.40	1.00	2.00	0.50	48	hoverfly
	Syrphidae	*Eristalis tenax*		1.40	1.08	2.15	**1.80**	97	hoverfly

(*continued on next page*)

Table 1 (*continued*)

Class	Order/Family	Species	Eye Type	BL (cm)	$\Delta\phi$ (deg)	$\Delta\rho$ (deg)	CPD	Ref.	Common Name
	Syrphidae	*Syritta pipiens*	NS	0.78	0.60	1.20	0.83	49	hoverfly
	Tephritidae	*Bactrocera tryoni*	NS	0.65	2.00	**1.72**	0.58	54	australian fruitfly
	Tipulidae	*Tipula pruinosa*	NS	1.43	5.80	11.60	0.09	48	cranefly
	Ephemeroptera								
	Ephemeridae	*Ephemera vulgata*	apposition	3.00	2.20	4.40	0.23	48	mayfly
	Leptophlebiidae	*Atalophlebia*	superposition	0.83	2.00	**2.00**	0.50	36	male mayfly
	Hemiptera								
	Aphalaridae	*Anoeconesossa bundoorensis*		0.20	5.70	11.40	0.09	24	aphid
	Aphalaridae	*Ctenarytaina bipartita*		0.14	6.30	12.60	0.08	24	aphid
	Aphalaridae	*Ctenarytaina eucalypti*		0.27	6.60	13.20	0.08	24	aphid
	Aphalaridae	*Glycaspis brimblecombei*		0.30	5.50	11.00	0.09	24	aphid
	Aphididae	*Acyrthosipehon pisum*	apposition	0.12	8.31	16.62	0.06	18	aphid
	Aphididae	*Aphis sambuci*	apposition	0.08	6.48	12.96	0.08	18	aphid
	Aphididae	*Brevicoryne brassicae*	apposition	0.08	8.51	17.02	0.06	18	aphid
	Aphididae	*Cavariella aegopodii*	apposition	0.06	8.41	16.82	0.06	18	aphid
	Aphididae	*Cinara pilicornis*	apposition	0.10	7.88	15.76	0.06	18	aphid
	Aphididae	*Drepanosiphum platanoidis*	apposition	0.11	5.18	10.36	0.10	18	aphid
	Aphididae	*Hyperomyzus lactucae*	apposition	0.08	7.99	15.98	0.06	18	aphid
	Aphididae	*Lachnus roboris*	apposition	0.15	7.33	14.66	0.07	18	aphid
	Aphididae	*Rhopalosiphum padi*	apposition	0.05	7.76	15.52	0.06	18	aphid
	Belostomatidae	*Lethocerus insulanus*	apposition	6.00	2.50	**6.50**	0.15	40	toebiter
	Belostomatidae	*Lethocerus* sp.	apposition	6.75		**9.00**	0.11	41	toebiter
	Gerridae	*Aquarius paludum*	apposition	1.20	2.10	4.20	0.24	48	water strider
	Gerridae	*Gerris lacustris*	apposition	0.90	0.55	1.10	0.91	16	water strider
	Notonectidae	*Notonecta glauca*	apposition	1.45	1.65	3.30	0.30	48	backswimmer
	Reduviidae	*Platymeris biguttatus*		2.50	3.70	**1.50**	0.67	88	assasain bug
	Hymenoptera								
	Andrenidae	*Perdita minima*	apposition	0.15	4.72	9.44	0.11	42	
	Andrenidae	*Protoxaea gloriosa*	apposition	0.95	1.68	3.36	0.30	42	
	Apidae	*Amegilla* sp.	apposition	1.15	1.00	2.00	0.50	48	
	Apidae	*Anthophora occidentalis*	apposition	0.85	1.71	3.42	0.29	42	
	Apidae	*Apis cerana*	apposition	0.09		**1.20**	0.83	91	
	Apidae	*Apis dorsata*	apposition	3.00		**1.80**	0.56	91	
	Apidae	*Apis florea*	apposition	0.10		**1.10**	0.91	91	
	Apidae	*Apis mellifera*	apposition	1.50	0.80	**2.60**	0.38	48	honeybee
	Apidae	*Apis mellifera*	apposition	1.50		**1.20**	0.83	49	honeybee
	Apidae	*Apis mellifera*	apposition	1.50		**1.60**	0.63	77	honeybee
	Apidae	*Bombus griseocollis*	apposition	1.20	1.53	3.06	0.33	42	
	Apidae	*Bombus impatiens*	apposition	1.30			**0.35**	55	bumble bee
	Apidae	*Bombus terrestris*	apposition	0.41	0.60	1.20	0.83	92	bumblebee
	Apidae	*Liotrigona madecassa*	apposition	0.15	3.87	7.74	0.13	42	
	Apidae	*Megaphragma mymaripenne*	apposition	0.02	21.50	43.00	0.02	56	parisitoid wasp
	Apidae	*Xylocopa californica*	apposition	1.36	1.38	2.76	0.36	42	
	Apidae	*Xylocopa latipes*	apposition	1.70	1.23	2.46	0.41	42	
	Apidae	*Xylocopa lecuothorax*	apposition	0.25	1.10	**0.80**	1.25	90	carpenter bee
	Apidae	*Xylocopa tenuiscapa*	apposition	0.25	1.00	**1.10**	0.91	90	indian carpenter bee
	Apidae	*Xylocopa tranquebarica*	apposition	0.25	0.80	**2.70**	0.37	90	carpenter bee
	Apidae	*Xylocopa varipuncta*	apposition	1.30	1.36	2.72	0.37	42	
	Crabronidae	*Bembix palmata*	apposition	1.70	0.41	0.82	1.22	48	sand wasp
	Formicidae	*Atta cephalotes*	apposition	0.95	0.26	0.52	1.92	1	leafcutter ant
	Formicidae	*Camponotus aethiops*	apposition	0.75	3.27	6.54	0.15	103	ant
	Formicidae	*Cataglyphis bicolor*	apposition	0.84	4.00	8.00	0.13	48	desert ant
	Formicidae	*Formica cunicularia*	apposition	0.53	2.59	5.18	0.19	103	ant
	Formicidae	*Melophorus bagoti*	apposition	0.99	3.70	**2.90**	0.34	85	Australian desert ant
	Formicidae	*Myrmecia gulosa*	apposition	2.25	1.70	3.40	0.29	48	giant bull ant
	Formicidae	*Myrmecia midas*	apposition	0.14			**0.57**	73	ant
	Formicidae	*Myrmecia tarsata*	apposition	0.23			**0.6**	70	ant
	Formicidae	*Polyrhachis sokolova*		1.10	5.90	11.80	0.08	69	intertidal ant
	Formicidae	*Temnothorax rugatulus*	apposition	0.32	16.80	33.60	0.03	75	ant
	Halictidae	*Augochlora pura*	apposition	0.45	2.72	5.44	0.18	42	
	Halictidae	*Lasioglossum inconspicuum*	apposition	0.22	3.37	6.74	0.15	42	
	Halictidae	*Lasioglossum noctivagum*	apposition	0.43	2.75	5.50	0.18	42	
	Halictidae	*Megalopta ecuadoria*	apposition	0.54	2.43	4.86	0.21	42	
	Halictidae	*Megalopta genalis*	apposition	0.75	2.05	4.10	0.24	42	
	Megachilidae	*Megachile campanulae*	apposition	0.59	1.75	3.50	0.29	42	
	Mymaridae	*Anaphes flavipes*	apposition	0.05	15.00	30.00	0.03	56	parisitoid wasp
	Tipulidae	*Tetragonula carbonaria*	apposition	0.11	1.56	3.12	0.32	20	
	Trichogrammatidae	*Trichogramma evanescens*	apposition	0.03	9.98	19.96	0.05	26	parisitoid wasp
	Vespidae	*Vespa vulgaris*	apposition	1.45	1.00	2.00	0.50	48	common yellowjacket
	Lepidoptera								
	Gracillariidae	*Cameraria ohridella*		0.50	7.10	14.20	0.07	27	leaf mining moth
	Hedylidae	*Macrosoma heliconiaria*	superposition	1.40	2.20	4.40	0.23	102	nocturnal butterfly
	Hesperiidae	*Hesperilla ornata*	superposition	1.90	1.60	3.20	0.31	35	skipper butterfly
	Hesperiidae	*Hesperilla picta*	superposition	1.40	1.60	3.20	0.31	35	skipper butterfly
	Hesperiidae	*Netrocoryne repanda*	superposition	1.50	2.00	4.00	0.25	35	skipper butterfly

Table 1 (*continued*)

Class	Order/Family	Species	Eye Type	BL (cm)	$\Delta\phi$ (deg)	$\Delta\rho$ (deg)	CPD	Ref.	Common Name
	Hesperiidae	*Ocybadistes walkeri*	superposition	1.00	1.90	3.80	0.26	35	skipper butterfly
	Hesperiidae	*Ocybadistes walkeri*	superposition	1.04	1.95	**2.18**	0.46	48	green grass dart skipper
	Hesperiidae	*Taractrocera papyria*	superposition	0.80	2.00	4.00	0.25	35	skipper butterfly
	Hesperiidae	*Toxidia peron*	superposition	1.40	1.90	3.80	0.26	35	skipper butterfly
	Hesperiidae	*Trapezites symmomus*	superposition	2.73	1.70	3.40	0.29	35	skipper butterfly
	Lycaenidae	*Curetis acuta*	apposition	1.64	1.04	2.08	0.48	94	
	Lycaenidae	*Jamides alecto*	apposition	1.50	1.34	2.68	0.37	94	
	Noctuidae	*Phalaenoides tristifica*	superposition	1.69	1.90	**1.58**	0.63	48	
	Nymphalidae	*Araschnia levana*		1.30	1.40	2.80	0.36	78	map butterfly
	Nymphalidae	*Argyreus hyperbius*	apposition	2.84	0.81	1.62	0.62	94	
	Nymphalidae	*Asterocampa leilia*		2.18	0.90	1.80	0.56	79	Empress Leilia
	Nymphalidae	*Caligo eurilochus*		3.10	0.77	1.54	0.65	78	forest giant owl
	Nymphalidae	*Caligo memnon*		3.80	1.00	**1.10**	0.91	28	owl butterfly
	Nymphalidae	*Cyrestis thyodamas*	apposition	1.47	1.20	2.40	0.42	94	
	Nymphalidae	*Euploea mulciber*	apposition	2.73	0.99	1.98	0.51	94	
	Nymphalidae	*Heteronympha merope*	apposition	2.10	1.25	**1.50**	0.67	48	common brown
	Nymphalidae	*Heteronympha merope*	apposition	2.10	1.40	**1.90**	0.53	49	
	Nymphalidae	*Hypolimnas bolina*	apposition	2.40	0.88	1.76	0.57	94	
	Nymphalidae	*Lethe europa*	apposition	1.94	0.88	1.76	0.57	94	
	Nymphalidae	*Melanitis leda*	apposition	1.14	1.44	**1.50**	0.67	48	evening brown butterfly
	Nymphalidae	*Morpho peleides*		3.81	1.00	**0.96**	1.04	28	blue morpho
	Nymphalidae	*Parantica aglea*	apposition	2.86	1.14	2.28	0.44	94	
	Nymphalidae	*Parthenos sylvia*		2.80	0.90	1.80	0.56	78	clipper
	Nymphalidae	*Penthema formosanum*	apposition	2.27	0.76	1.52	0.66	94	
	Nymphalidae	*Polygonia c-album*		0.98	1.30	2.60	0.38	78	comma
	Nymphalidae	*Precis almana*	apposition	1.89	0.81	1.62	0.62	94	
	Papilionidae	*Battus philenor*		3.51	0.70	1.40	0.71	9	pipevine swallowtail
	Papilionidae	*Papilio machaon*	apposition	2.10	0.90	1.80	0.56	48	old world swallowtail
	Pieridae	*Appias lyncida*	apposition	1.80	0.99	1.98	0.51	94	
	Pieridae	*Colias eurytheme*	apposition	1.49	0.72	1.44	0.69	59	orange sulphur
	Pieridae	*Pieris brassicae*	apposition	2.70	1.80	3.60	0.28	48	cabbage butterfly
	Pyralidae	*Ephestia kuehniella*	superposition	1.20	2.50	5.00	0.20	34	Mediterranean flour moth
	Pyralidae	*Ephestia kuehniella*	superposition	1.20	3.00	6.00	0.17	48	flour moth
	Sphingidae	*Deilephila elpenor*	superposition	3.58	1.12	**4.04**	0.25	95	
	Sphingidae	*Macroglossum stellatarum*	superposition	2.14		**1.30**	0.77	21	hummingbird hawkmoth
	Sphingidae	*Macroglossum stellatarum*	superposition	2.14	1.30	**1.75**	0.57	95	
	Sphingidae	*Manduca sexta*	superposition	4.84	0.91	**3.26**	0.31	95	
	Mantodea								
	Liturgusidae	*Ciulfina biseriata*	apposition	2.50	0.80	1.60	0.63	48	praying mantis
	Mantidae	*Orthodera ministralis*	apposition	4.00	1.20	2.40	0.42	48	garden mantis
	Mantidae	*Tenodera australasiae*	apposition	8.00	0.60	**0.60**	1.67	48	purple winged mantis
	Mecoptera								
	Panorpidae	*Panorpa dubia*	apposition	2.01	6.00	12.00	0.08	14	scorpion fly
	Megaloptera								
	Sialidae	*Sialis flavilatera*	apposition	1.24	2.40	4.80	0.21	48	alderfly
	Neuroptera								
	Ascalaphidae	*Ascalaphus* sp.	superposition	5.00	1.40	2.80	0.36	48	owlfly
	Ascalaphidae	*Libelloides macaronius*	superposition	2.90	1.10	**1.40**	0.71	8	owlfly
	Mantispidae	*Mantispa styriaca*	superposition	0.50	1.80	**2.0**	0.28	22	mantis fly
	Odonata								
	Aeshnidae	*Aeshna grandis*	apposition	7.30	0.80	1.60	0.63	48	brown hawker dragonfly
	Aeshnidae	*Aeshna palmata (adult)*	apposition	6.85	0.24	0.48	2.08	89	paddletail darter dragonfly
	Aeshnidae	*Aeshna palmata (larva)*	apposition	4.00	0.45	0.90	1.11	87	
	Aeshnidae	*Anax junius (adult)*	apposition	7.40	0.24	0.48	2.08	48	common green darter dragonfly
	Aeshnidae	*Anax junius (larva)*	apposition	4.50	0.45	0.90	1.11	87	
	Coenagrionidae	*Megalagrion blackburni*	apposition	4.85	0.63	1.25	0.80	80	damselfly
	Coenagrionidae	*Megalagrion calliphya*	apposition	3.25	0.77	1.53	0.65	80	damselfly
	Coenagrionidae	*Megalagrion hawaiiense*	apposition	3.59	0.78	1.57	0.64	80	damselfly
	Coenagrionidae	*Megalagrion heterogamias*	apposition	4.02	0.73	1.47	0.68	80	damselfly
	Coenagrionidae	*Megalagrion koelense*	apposition	2.35	0.78	1.56	0.64	80	damselfly
	Coenagrionidae	*Megalagrion leptodemas*	apposition	3.13	0.80	1.60	0.63	80	damselfly
	Coenagrionidae	*Megalagrion nigrohamatum nigrohamatum*	apposition	4.41	0.57	1.15	0.87	80	damselfly
	Coenagrionidae	*Megalagrion nigrohamatum nigrohamatum*	apposition	3.22	0.66	1.32	0.76	80	damselfly
	Coenagrionidae	*Megalagrion oahuense*	apposition	4.24	0.93	1.86	0.54	80	damselfly
	Coenagrionidae	*Megalagrion oceanicum*	apposition	3.77	0.70	1.41	0.71	80	damselfly
	Coenagrionidae	*Megalagrion oresitrophum*	apposition	2.61	0.83	1.66	0.60	80	damselfly
	Coenagrionidae	*Megalagrion vagabundum*	apposition	3.44	0.76	1.52	0.66	80	damselfly
	Coenagrionidae	*Megalagrion xanthomelas*	apposition	3.50	0.82	1.65	0.61	84	orangeback damselfly
	Coenagrionidae	*Xanthagrion erythroneurum*	apposition	2.30	1.20	2.40	0.42	48	red and blue damselfly
	Corduliidae	*Hemicordulia tau*	apposition	5.00	0.90	**1.40**	0.71	48	emerald tau dragonfly
	Corduliidae	*Somatochlora albicincta (larva)*	apposition	2.18	1.73	3.46	0.29	87	
	Gomphidae	*Austrogomphus guerini*	apposition	5.08	0.58	1.16	0.86	48	yellow striped hunter dragonfly

(*continued on next page*)

Table 1 (*continued*)

Class	*Order/Family*	*Species*	*Eye Type*	*BL* (cm)	$\Delta\phi$ (deg)	$\Delta\rho$ (deg)	CPD	*Ref.*	*Common Name*
	Libellulidae	*Sympetrum striolatum*	apposition	4.05	0.40	0.80	1.25	48	common darter dragonfly
	Libellulidae	*Sympetrum striolatus*	apposition	4.30	0.30	0.60	1.67	45	dragonfly
	Libellulidae	*Zyxomma obtusum*	apposition	3.70	0.65	1.30	0.77	48	duskdarter dragonfly
	Orthoptera								
	Acrididae	*Locusta migratoria*	apposition	4.00	0.90	1.80	0.56	48	locust
	Phasmida								
	Lonchodidae	*Carausius morosus*	apposition	9.00	7.50	15.00	0.07	48	stick insect
	Strepsiptera								
	Xenidae	*Xenos vesparum*		0.28	9.00	**50.00**	0.02	74	
Ichthyostraca	**Arguloida**								
	Argulidae	*Argulus coregoni*	apposition	1.10	13.20	26.40	0.04	67	fish louse
	Argulidae	*Argulus foliaceus*	apposition	0.65	16.75	33.50	0.03	67	fish louse
Malacostraca	**Amphipoda**								
	Brachyscelidae	*Brachyscelus* sp.	apposition	1.00	1.40	**6.30**	0.16	47	
	Cystisomatidae	*Cystisoma* sp.	apposition	14.00	0.65	**3.90**	0.26	47	
	Dulichiidae	*Dyopedos porrectus*	apposition	0.65	6.00	12.00	0.08	66	stalk inhabiting amphipod
	Eupronoidae	*Parapronoe crustulum*	apposition	2.00	1.10	2.20	0.45	47	
	Hyalidae	*Parhyale hawaiensis*	apposition	1.00	15.00	**15.00**	0.07	76	
	Hyperiidae	*Themisto compressa*	apposition	1.50	1.50	**4.50**	0.22	47	
	Lestrigonidae	*Lestrigonus* sp.	apposition	0.30	3.50	**10.50**	0.10	47	
	Oxycephalidae	*Streetsia challengeri*	apposition	3.50	0.32	**6.40**	0.16	47	
	Paraphronimidae	*Paraphronima gracilis*	apposition	1.10	1.20	**2.50**	0.40	25	
	Phronimidae	*Phronima sedentaria*	apposition	1.50	0.25	**2.30**	0.43	47	parasitic hyperiid amphipod
	Phronimidae	*Phronima* sp.	apposition	3.00	0.44	**3.50**	0.29	46	
	Phrosinidae	*Phrosina semilunata*	apposition	2.00	0.60	**4.80**	0.21	47	
	Platyscelidae	*Platyscelus ovoides*	apposition	2.00	1.20	**3.60**	0.28	47	
	Thamneidae	*Thamneus* sp.	apposition	0.68	4.80	**4.80**	0.21	47	
	Decapoda								
	Benthesicymidae	*Gennadas* sp.	superposition	0.32	2.90	5.80	0.17	63	
	Cambaridae	*Procambarus clarkii*	superposition	9.00		**2.70**	0.37	30	red swamp crayfish
	Carcinidae	*Carcinus maenas*	apposition	3.00			**0.51**	106	green shore crab
	Crangonidae	*Crangon septemspinosa*		7.00	3.78	7.56	0.13	33	sand shrimp
	Crangonidae	*Neocrangon abyssorum*		1.85	2.00	4.00	0.25	33	
	Crangonidae	*Neocrangon resima*		3.70	3.25	6.50	0.15	33	
	Dotillidae	*Scopimera inflata*	apposition	1.30			**1.08**	106	sand bubbler crab
	Glyphocrangonidae	*Glyphocrangon aculeata*		10.20	0.92	1.84	0.54	33	
	Glyphocrangonidae	*Glyphocrangon alispina*		10.80	0.97	1.94	0.52	33	
	Glyphocrangonidae	*Glyphocrangon longirostris*		10.60	0.95	1.90	0.53	33	
	Glyphocrangonidae	*Glyphocrangon longleyi*		6.10	1.03	2.06	0.49	33	
	Grapsidae	*Leptograpsus variegatus*	apposition	5.00		**1.50**	0.67	96	purple rock crab
	Grapsidae	*Leptograpsus variegatus*	apposition	5.00			**0.74**	106	purple rock crab
	Grapsidae	*Pachygrapsus marmoratus*	apposition	4.00			**0.50**	106	marbled rock crab
	Heloeciidae	*Heloecius cordiformis*	apposition	1.80			**0.87**	106	
	Hippolytidae	*Hippolyte californiensis*	apposition	2.80		**1.50**	0.67	5	
	Lithodidae	*Paralomis multispina*	apposition	8.00	3.00	6.00	0.17	23	king crab
	Macrophthalmidae	*Macrophthalmus (Mareotis) setosus*	apposition	3.05			**1.06**	106	mudflat sentinal crab
	Mictyridae	*Mictyris longicarpus*	apposition	2.00			**1.23**	106	light blue soldier crab
	Munididae	*Munida rugosa*	superposition	10.00		**6.58**	0.15	86	rugose squat lobster
	Nephropidae	*Homarus americanus*	superposition	25.00	1.30	2.60	0.38	33	american lobster
	Nephropidae	*Nephrops norvegicus*	superposition	25.00	0.97	**8.62**	0.12	33, 86	norway lobster
	Ocypodidae	*Austruca lactea*	apposition	1.70			**1.30**	105	fiddler crab
	Ocypodidae	*Gelasimus dampieri*	apposition	1.95			**1.92**	2	fiddler crab
	Ocypodidae	*Leptuca pugilator*	apposition	1.40	1.00		**1.04**	52	fiddler crab
	Ocypodidae	*Minuca pugnax*	apposition	3.00	2.05	4.10	0.24	15	fiddler crab
	Ocypodidae	*Ocypode ceratophthalmus*	apposition	3.50	0.23	1.0	**1.57**	19	ghost crab
	Ocypodidae	*Ocypode ceratophthalmus*	apposition	2.50			**1.93**	106	horned ghost crab
	Ocypodidae	*Ocypode cordimana*	apposition	2.70			**0.95**	106	smooth handed ghost crab
	Ocypodidae	*Tubuca flammula*	apposition	3.13			**1.99**	2	fiddler crab
	Ocypodidae	*Uca* sp.	apposition	1.75			**1.24**	106	fiddler crab
	Palaemonidae	*Actinimenes inornatus*		0.24	3.53	7.06	0.14	17	shrimp
	Palaemonidae	*Actinimenes ornatus*		0.18	3.16	6.32	0.16	17	shrimp
	Palaemonidae	*Anchistus custos*		0.96	4.96	9.92	0.10	17	shrimp
	Palaemonidae	*Ancylomenes holthuisi*		0.48	4.58	9.16	0.11	17	shrimp
	Palaemonidae	*Ancylomenes pedersoni*		0.22		**8.20**	0.10	13	shrimp
	Palaemonidae	*Ancylomenes tosaensis*		0.36	3.94	7.88	0.13	17	shrimp
	Palaemonidae	*Ancylomenes venustus*		0.51	4.95	9.90	0.10	17	shrimp
	Palaemonidae	*Balssia gasti*		0.17	4.96	9.92	0.10	17	shrimp
	Palaemonidae	*Brucecaris tenuis*		0.23	5.02	10.04	0.10	17	shrimp
	Palaemonidae	*Cainonia medipacifica*		0.53	6.57	13.14	0.08	17	shrimp
	Palaemonidae	*Conchodytes biunguiculatus*		0.60	5.62	11.24	0.09	17	shrimp
	Palaemonidae	*Conchodytes nipponensis*		1.02	4.18	8.36	0.12	17	shrimp
	Palaemonidae	*Conchodytes placunae*		0.85	5.82	11.64	0.09	17	shrimp
	Palaemonidae	*Conchodytes_meleagrinae*		0.60	5.10	10.20	0.10	17	shrimp
	Palaemonidae	*Coralliocaris superba*		0.23	2.60	5.20	0.19	17	shrimp

Table 1 (*continued*)

Class	Order/Family	Species	Eye Type	BL (cm)	$\Delta\phi$ (deg)	$\Delta\rho$ (deg)	CPD	Ref.	Common Name
	Palaemonidae	*Coralliocaris viridis*		0.33	2.70	5.40	0.19	17	shrimp
	Palaemonidae	*Cristimenes commensalis*		0.13	4.17	8.34	0.12	17	shrimp
	Palaemonidae	*Cuapetes americanus*	superposition	0.19	3.47	6.94	0.14	17	shrimp
	Palaemonidae	*Cuapetes andamanensis*		0.33	3.09	6.18	0.16	17	shrimp
	Palaemonidae	*Cuapetes elegans*	superposition	0.33	2.76	5.52	0.18	17	shrimp
	Palaemonidae	*Cuapetes ensifrons*		0.26	2.97	5.94	0.17	17	shrimp
	Palaemonidae	*Cuapetes grandis*		0.20	4.03	8.06	0.12	17	shrimp
	Palaemonidae	*Cuapetes kororensis*		0.37	3.82	7.64	0.13	17	shrimp
	Palaemonidae	*Cuapetes tenuipes*		0.41	2.86	5.72	0.17	17	shrimp
	Palaemonidae	*Dactylonia okai*		0.15	5.93	11.86	0.08	17	shrimp
	Palaemonidae	*Fennera chacei*		0.09	7.15	14.30	0.07	17	shrimp
	Palaemonidae	*Hamodactylus boschmai*		0.11	4.04	8.08	0.12	17	shrimp
	Palaemonidae	*Hamopontonia corallicola*		0.35	5.98	11.96	0.08	17	shrimp
	Palaemonidae	*Harpiliopsis beaupresii*		0.17	4.03	8.06	0.12	17	shrimp
	Palaemonidae	*Harpiliopsis spinigera*		0.43	3.19	6.38	0.16	17	shrimp
	Palaemonidae	*Harpilius bayeri*		0.25	4.39	8.78	0.11	17	shrimp
	Palaemonidae	*Harpilius consobrinus*		0.23	3.74	7.48	0.13	17	shrimp
	Palaemonidae	*Holthuisaeus bermudensis*		0.32	8.33	16.66	0.06	17	shrimp
	Palaemonidae	*Ischnopontonia lophos*		0.14	6.56	13.12	0.08	17	shrimp
	Palaemonidae	*Laomenes amboinensis*		0.22	2.86	5.72	0.17	17	shrimp
	Palaemonidae	*Laomenes ceratophthalmus*		0.23	3.82	7.64	0.13	17	shrimp
	Palaemonidae	*Laomenes cornutus*		0.17	3.82	7.64	0.13	17	shrimp
	Palaemonidae	*Laomenes nudirostris*		0.43	2.99	5.98	0.17	17	shrimp
	Palaemonidae	*Lysmata amboinensis*		5.50		**5.60**	0.18	13	clearner shrimp
	Palaemonidae	*Macrobrachium rosenbergii*	superposition	33.00	1.75	3.50	0.29	58	freshwater prawn
	Palaemonidae	*Manipontonia psamathe*		0.18	4.58	9.16	0.11	17	shrimp
	Palaemonidae	*Neoanchistus nasalis*		0.59	5.41	10.82	0.09	17	shrimp
	Palaemonidae	*Neopontonides chacei*		0.11	4.81	9.62	0.10	17	shrimp
	Palaemonidae	*Odontonia katoi*		0.14	8.33	16.66	0.06	17	shrimp
	Palaemonidae	*Onycocaris quadratophthalma*		0.14	10.61	21.22	0.05	17	shrimp
	Palaemonidae	*Onycocaris* sp.		0.17	11.34	22.68	0.04	17	shrimp
	Palaemonidae	*Orthopontonia ornata*		0.27	5.73	11.46	0.09	17	shrimp
	Palaemonidae	*Palaemonella holmesi*		0.29	3.43	6.86	0.15	17	shrimp
	Palaemonidae	*Palaemonella pottsi*		0.16	5.46	10.92	0.09	17	shrimp
	Palaemonidae	*Palaemonella spinulata*		0.14	4.17	8.34	0.12	17	shrimp
	Palaemonidae	*Paranchistus pycnodontae*		0.45	4.44	8.88	0.11	17	shrimp
	Palaemonidae	*Periclimenaeus ascidiarum*		0.16	7.88	15.76	0.06	17	shrimp
	Palaemonidae	*Periclimenaeus bredini*		0.56	9.47	18.94	0.05	17	shrimp
	Palaemonidae	*Periclimenaeus caraibicus*		0.21	5.21	10.42	0.10	17	shrimp
	Palaemonidae	*Periclimenaeus hecate*		0.36	5.21	10.42	0.10	17	shrimp
	Palaemonidae	*Periclimenaeus maxillulidens*		0.17	10.37	20.74	0.05	17	shrimp
	Palaemonidae	*Periclimenaeus orbitocarinatus*		0.15	8.20	16.40	0.06	17	shrimp
	Palaemonidae	*Periclimenaeus storchi*		0.23	6.98	13.96	0.07	17	shrimp
	Palaemonidae	*Periclimenella spinifera*		0.27	3.37	6.74	0.15	17	shrimp
	Palaemonidae	*Periclimenes gonioporae*		0.16	5.27	10.54	0.09	17	shrimp
	Palaemonidae	*Periclimenes harringtoni*		0.23	9.17	18.34	0.05	17	shrimp
	Palaemonidae	*Periclimenes incertus*		0.13	4.30	8.60	0.12	17	shrimp
	Palaemonidae	*Periclimenes iridescens*		0.14	5.73	11.46	0.09	17	shrimp
	Palaemonidae	*Periclimenes madreporae*		0.14	4.58	9.16	0.11	17	shrimp
	Palaemonidae	*Periclimenes patae*		0.16	3.62	7.24	0.14	17	shrimp
	Palaemonidae	*Periclimenes rathbunae*		0.35	4.09	8.18	0.12	17	shrimp
	Palaemonidae	*Periclimenes scriptus*		0.13	6.25	12.50	0.08	17	shrimp
	Palaemonidae	*Periclimenes yucatanicus*		0.23	4.98	9.96	0.10	17	shrimp
	Palaemonidae	*Phycomenes indicus*		0.21	3.64	7.28	0.14	17	shrimp
	Palaemonidae	*Phycomenes siankaanensis*		0.23	4.09	8.18	0.12	17	shrimp
	Palaemonidae	*Phycomenes zostericola*		0.16	6.03	12.06	0.08	17	shrimp
	Palaemonidae	*Platypontonia hyotis*		0.52	5.26	10.52	0.10	17	shrimp
	Palaemonidae	*Pontonia margarita*		0.45	6.07	12.14	0.08	17	shrimp
	Palaemonidae	*Pontonia mexicana*	superposition	0.83	8.19	16.38	0.06	17	shrimp
	Palaemonidae	*Pontonia panamica*		0.55	9.80	19.60	0.05	17	shrimp
	Palaemonidae	*Pontonia pinnophylax*		0.90	8.52	17.04	0.06	17	shrimp
	Palaemonidae	*Pontonides loloata*		0.09	2.55	5.10	0.20	17	shrimp
	Palaemonidae	*Pontoniopsis comanthi*		0.13	3.53	7.06	0.14	17	shrimp
	Palaemonidae	*Thaumastocaris streptopus*		0.55	3.34	6.68	0.15	17	shrimp
	Palaemonidae	*Typton gnathophylloides*		0.12	7.16	14.32	0.07	17	shrimp
	Palaemonidae	*Typton hephaestus*		0.26	8.81	17.62	0.06	17	shrimp
	Palaemonidae	*Typton holthuisi*		0.13	7.29	14.58	0.07	17	shrimp
	Palaemonidae	*Typton tortugae*		0.19	7.33	14.66	0.07	17	shrimp
	Palaemonidae	*Urocaridella antonbruuni*		2.80		**7.20**	0.14	13	cleaner shrimp
	Palaemonidae	*Urocaris longicaudata*		0.29	4.57	9.14	0.11	17	shrimp
	Palaemonidae	*Vir philippinensis*		0.15	3.82	7.64	0.13	17	shrimp
	Palinuridae	*Panulirus interruptus*	superposition	30.00	2.43	4.86	0.21	33	california spiny lobster
	Pandalidae	*Heterocarpus hostilis*		2.40	1.61	3.22	0.31	33	
	Pandalidae	*Heterocarpus vicarius*		11.00	1.68	3.36	0.30	33	northern nylon shrimp
	Pandalidae	*Pandalus amplus*	superposition	16.40	1.71	3.42	0.29	33	deep water big eye

(*continued on next page*)

Table 1 (*continued*)

Class	*Order/Family*	*Species*	*Eye Type*	*BL* (cm)	*Δϕ* (deg)	*Δρ* (deg)	CPD	*Ref.*	*Common Name*
	Pandalidae	*Pandalus danae*	superposition	11.00	1.61	3.22	0.31	33	dock shrimp/coon-stripe shrimp
	Pandalidae	*Pandalus dispar*	superposition	17.00	1.62	3.24	0.31	33	sidestriped shrimp
	Pandalidae	*Pandalus goniurus*	superposition	6.20	1.86	3.72	0.27	33	humphry shrimp/flexed pandalid
	Pandalidae	*Pandalus platyceros*	superposition	22.00	1.28	2.56	0.39	33	california spot prawn
	Parastacidae	*Cherax destructor*	superposition	20.00		**4.50**	0.22	11	common yabby/freshwater crayfish
	Portunidae	*Callinectes sapidus*	apposition	50.00		**1.80**	0.56	3	blue crab
	Scyllaridae	*Scyllarides latus*	apposition	35.00	3.80	7.60	0.13	53	Mediterranian slipper lobster
	Sergestidae	*Allosergestes pectinatus*		2.45	4.25	8.50	0.12	109	
	Sergestidae	*Deosergestes henseni*		4.20	2.95	5.90	0.17	109	
	Sergestidae	*Parasergestes armatus*		3.20	5.4	10.80	0.09	109	
	Sesarmidae	*Parasesarma erythodactylum*	apposition	2.00			**0.60**	106	
	Varunidae	*Neohelice granulata*		2.80			**1.93**	2	rock crab
	Varunidae	*Neohelice granulata*		2.90	0.40		**1.20**	10	crab
	Euphausiacea								
	Euphausiidae	*Euphausia gibboides*	superposition	2.10	2.60	5.20	0.19	32	
	Euphausiidae	*Euphausia pacifica*	superposition	1.65	3.00	6.00	0.17	32	
	Euphausiidae	*Euphausia superba*	superposition	5.25	2.30	4.60	0.22	32	
	Euphausiidae	*Stylocheiron maximum*	superposition	2.50	1.20	2.40	0.42	49	
	Euphausiidae	*Thysanopoda acutifrons*	superposition	3.95	3.70	7.40	0.14	32	
	Euphausiidae	*Thysanopoda cornuta*	superposition	7.65	3.40	6.80	0.15	32	
	Euphausiidae	*Thysanopoda cristata*	superposition	5.00	2.60	5.20	0.19	32	
	Euphausiidae	*Thysanopoda egregia*	superposition	7.65	5.10	10.20	0.10	32	
	Euphausiidae	*Thysanopoda monacantha*	superposition	3.00	3.60	7.20	0.14	32	
	Euphausiidae	*Thysanopoda pectinata*	superposition	3.65	3.80	7.60	0.13	32	
	Euphausiidae	*Thysanopoda tricuspidata*	superposition	2.00	2.90	5.80	0.17	32	
	Euphausiidae	*Thysanopoda tricuspidata*	apposition	2.20	4.50	9.00	0.11	64	
	Isopoda								
	Cirolanidae	*Natatolana borealis*	apposition	1.00	10.00	20.00	0.05	71	
	Lophogastrida								
	Gnathophausiidae	*Neognathophausia ingens*	superposition	4.28	1.80	3.60	0.28	101	
	Mysida								
	Mysidae	*Dioptromysis paucispinosa*	superposition	0.50	0.64	1.28	0.78	49	
	Mysidae	*Euchaetomera typica*	superposition	0.93	1.50	3.00	0.33	29	
	Stomatopoda								
	Gonodactylidae	*Gonodactylus chiragra*	apposition	8.00			**0.80**	57	mantis shrimp
	Gonodactylidae	*Gonodactylus* spp.	apposition	5.00		**0.57**	1.75	83	mantis shrimp
	Hemisquillidae	*Hemisquilla californiensis*	apposition	22.00			**1.10**	57	mantis shrimp
	Lysiosquillidae	*Lysiosquilla scabricauda*	apposition	30.00		**0.91**	1.10	81	mantis shrimp
	Lysiosquillidae	*Lysiosquilla tredecimdentata*	apposition	11.00			**1.50**	57	mantis shrimp
	Nannosquillidae	*Coronis scolopendra*	apposition	7.00			**1.00**	57	mantis shrimp
	Nannosquillidae	*Coronis scolopendra*	apposition	4.50		**0.89**	1.12	81	mantis shrimp
	Odontodactylidae	*Odontodactylus scyllarus*	apposition	14.00			**1.10**	57	mantis shrimp
	Protosquillidae	*Echinosquilla guerinii*	apposition	8.10		**1.03**	0.97	83	mantis shrimp
	Pseudosquillidae	*Pseudosquilla ciliata*	apposition	3.00		**0.64**	1.56	83	mantis shrimp
	Squillidae	*Crenatosquilla oculinova*	apposition	2.00		**2.30**	0.43	82	mantis shrimp
	Squillidae	*Oratosquillina inornata*	apposition	14.00			**0.60**	57	mantis shrimp
	Squillidae	*Squilla empusa*	apposition	30.00		**2.08**	0.48	83	mantis shrimp
	Squillidae	*Squilla mantis*	apposition	15.70		**2.20**	0.45	83	mantis shrimp
Merostomata	**Xiphosurida**								
	Limulidae	*Limulus polyphemus*	apposition	13.60			**0.23**	4	horseshoe crab
	‡Eurypterida	*Pterygotus anglicus*		250.00	0.77	1.54	0.65	107	EXTINCT
		Erettopterus osiliensis		100.00	1.14	2.28	0.44	107	EXTINCT
		Slimonia acuminata		100.00	1.44	2.88	0.35	107	EXTINCT
		Jaekelopterus rhenaniae		250.00	0.76	1.52	0.66	107	EXTINCT
		Eurypterus sp.		100.00	0.87	1.70	0.57	107	EXTINCT
		Acutiramus cummingsi		165.00	1.50	3.00	0.33	107	EXTINCT
Dinocaridida	**Radiodonta**								
	‡Anomaocarida	*Unknown*		70.00	1.40	2.80	0.36	108	EXTINCT
Ostracoda	**Myodocopida**								
	Cypridinidae	*Macrocypridina castanea*	apposition	0.50	6.00	12.00	0.08	51	
	Myodocopida								
	Philomedidae	*Pleoschisma agilis*	apposition	0.10	8.00		**0.06**	93	ostracod

acuity value currently described is 1.75 CPD, which is attributed to mantis shrimp (Stomatopoda, *Gonodactylus* spp.).

Given the availability of molecular data in online repositories, only a subset of total species in this database could be represented in our molecular phylogeny. For species in the database without accompanying molecular data, molecular data from a species within the same genus was used to determine the placement in the larger tree. All instances of this curation to the level of genus are summarized in Table S3. The result yielded a trimmed subset of 278 genera represented by both the database and the phylogeny for subsequent analysis (phylogeny subset; Fig. 1, Fig. S2; Table S3), plus two larval dragonfly data points.

Table 2
Summary of phylogenetic generalized least-squares multivariate models of compound eye visual acuity (CPD). *ΔAIC*, calculated values correspond to best fit model; w_i, model probability; M, environmental media; L, light environment; H, horizon/visual scene structure; F, foraging strategy; B, body length.

Model	ΔAIC	w_i
M + L + F	0.00	0.50
M + L + H + F	0.37	0.42
M + F	5.26	0.04
M + H + F	6.43	0.02
M + L	7.04	0.01
M + L + H	7.72	0.01
L + F	20.80	0.00
L + H + F	22.89	0.00
F	24.97	0.00
H + F	27.03	0.00
M	30.90	0.00
M + H	30.92	0.00
L	31.98	0.00
L + H	34.02	0.00
NULL	37.25	0.00
H	39.06	0.00
B + L + F	448.52	0.00
B + M + L + F	448.79	0.00
B + F	448.91	0.00
B	449.12	0.00
B + L	449.40	0.00
B + M + F	450.41	0.00
B + M + L	451.30	0.00
B + L	451.90	0.00
B + H	456.58	0.00
B + H + F	456.73	0.00
B + M + H	457.48	0.00
B + L + H + F	457.89	0.00
B + M + L + H + F	458.55	0.00
B + M + H + F	458.67	0.00
B + M + L + H	460.65	0.00
B + L + H	460.70	0.00

3.3. Ecological patterns and predictors of compound eye acuity

3.3.1. Ecological factors

The PGLS analysis yielded two linear models of ecological factors that best predict variation in arthropod visual acuity. Of these two, the best-fit model ($\Delta AIC = 0.00$) incorporated environmental medium, foraging strategy, and environmental light intensity as the strongest co-predictors of CPD ($w_i = 0.50$; Table 2). The addition of visual scene structure information (horizon) also created an acceptable model ($\Delta AIC = 0.37$; $w_i = 0.42$; Table 2), though this model performs with slightly less weight than the best-fit model. The residuals from this analysis met our assumptions that the data were a good fit for the output models (Fig. S3).

When we compare the phylogeny subset visual acuity data across the categories of each ecological predictor, we find that CPD varies significantly within the categories of environmental medium (Kruskal-Wallace, $\chi^2 = 14.86$, df = 2, $p < 0.008$, Bonferroni corrected; Fig. 2A) and foraging strategy ($\chi^2 = 36.80$, df = 2, $p < 0.008$; Fig. 2B), but not for environmental light intensity (Wilcoxon, $W = 9608$, $p = 0.011$; Fig. 2C) or visual scene structure (Wilcoxon, $W = 4508$, $p = 0.34$; Fig. 2D). As predicted, animals primarily inhabiting water have significantly lower acuities than those in air (Dunn post hoc, $p < 0.008$), though the acuity of amphibious eyes that see in both water and air did not significantly differ from either the air or water group (Dunn post hoc; air/both, $p = 0.36$; water/both, $p = 0.03$; Figs. 2A and 3). Acuity was also much higher in active predators than non-active predators (Dunn post hoc test, ambush/other, $p < 0.008$; pursuit/other, $p < 0.008$; Fig. 2B), though visual acuity is similar between different active predation strategies (Dunn post hoc; ambush/pursuit, $p = 0.39$; Fig. 2B).

3.3.2. Body length

Our phylogenetically-corrected modeling results found that body length was not a significant predictor of acuity across diverse arthropod lineages, both alone and in all combinations with other co-factors ($\Delta AIC > 4$; Table 2). This stands in contrast to the weak, though significant, linear relationship observed between log transformed acuity CPD values and log transformed body length prior to running the PGLS ($R^2 = 0.31$; $p = 2.26e\text{-}16$; Fig. 3; Fig. S4). Since the uncorrected linear model (R^2) only explains 31% of the variation around the mean visual acuity (response variable), it is likely that body size is strongly associated with phylogeny, and thereby significance is lost with phylogenetic correction.

3.3.3. Eye type

Lastly, eye type descriptions (apposition, neural superposition and superposition) could only be acquired for 210 species in our phylogeny subset data, resulting in their exclusion from the PGLS analysis. A comparison of eye type without phylogenetic correction suggests that acuity does not significantly vary among eye types (Kruskal–Wallis, $\chi^2 = 5.71$; $p = 0.06$; Fig. 2E).

3.4. CPD visualization with AcuityView

Accounting for the full range of visual acuities represented in Fig. 3, we used *AcuityView* software to generate example image outputs for the best, worst, and median acuity values. These values cover approximately three orders of magnitude, represented by the robberfly, *Holcocephala abdominalis* (3.70 CPD), the springtail, *Dicyrtomina ornata* (0.02 CPD), and the water-flea, *Polyphemus pediculus* (0.25 CPD), respectively. In all three examples, spatial resolution of vision diminishes with distance (Fig. 4). To produce outputs that approximate the range of visual acuities represented in our database, the position of the viewer was set across three orders of magnitude of distance relative to the mean body length of all species, which was calculated as ~3 cm. For the species with the worst acuity, *D. ornata*, and median acuity, *P. pediculus*, spatial information is apparently lost at distances of 30 and 300 cm, respectively. Though these images are output as solid grey, with no visual information present, *Acuityview* is unable to account for visual processes that occur downstream from the retina, such as edge enhancement. Therefore, it is possible that in cases where all spatial information has been lost, the animal may still perceive some edges or areas of increased contrast.

4. Discussion

4.1. Database meta-analysis and limitations

There is a large body of research that establishes the impact of ecological factors on the evolution of compound eye visual acuity (for excellent reviews see Land and Nilsson, 2002; Cronin et al., 2014). Here, we provide a comprehensive test for interactions among multiple, independent factors on the evolution of acuity in compound eyes, using a phylogenetic distribution of Arthropoda. We conclude from our analysis that foraging strategy, environmental light intensity, and the environmental medium are the strongest predictors of visual acuity in arthropods. There is also support that a fourth factor - the horizontal structure of the environmental light field - is associated with compound eye acuity, though not as strongly as the other co-factors. From the trends in our boxplot comparisons, we can infer that the interplay of active predation foraging strategies, bright light environments, an air medium, and a horizon dominant visual scene together select for higher resolving visual systems. Indeed, the top two visual acuities reported for compound eyes (robberflies and dragonflies)

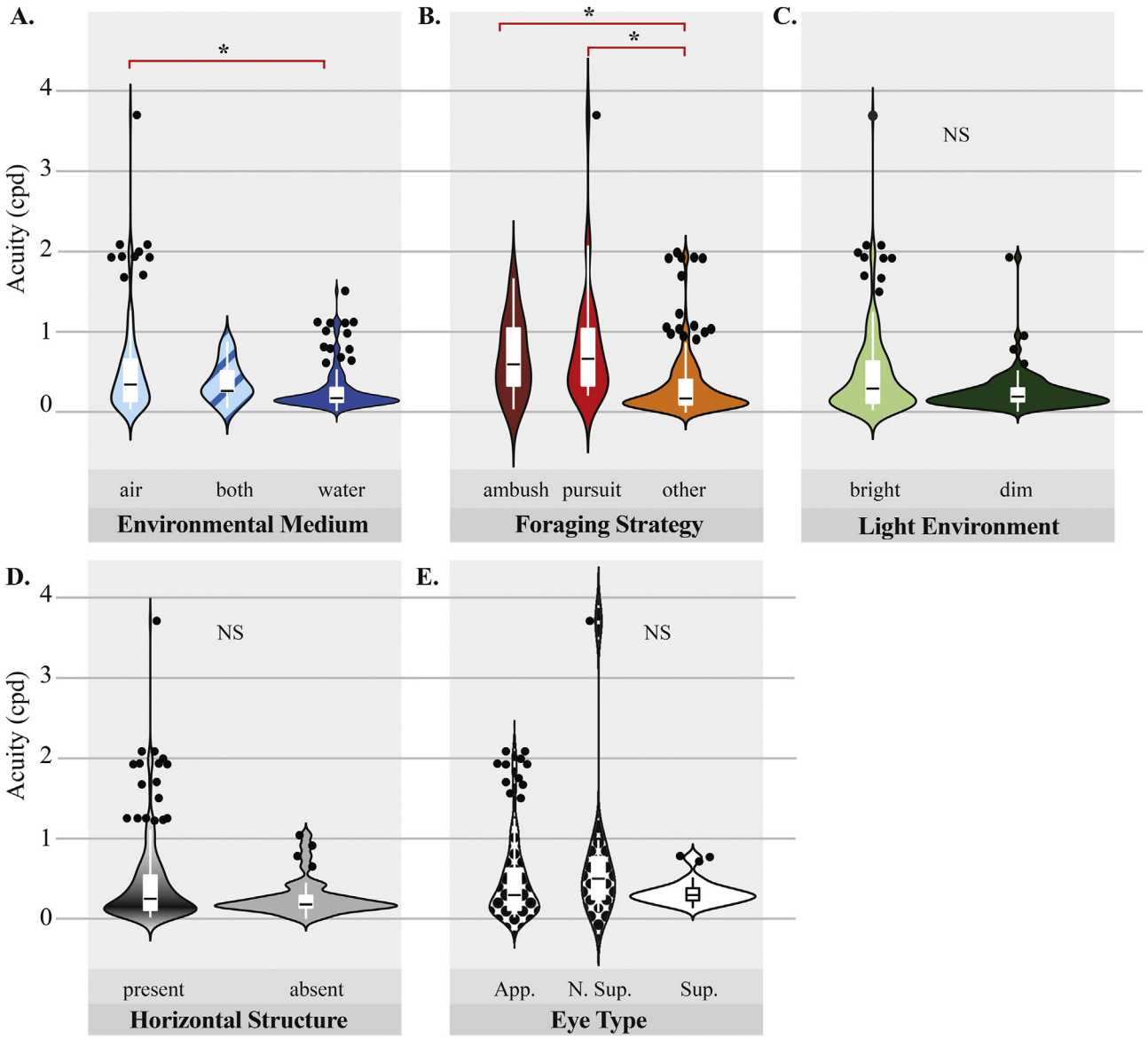

Fig. 2. Comparison of CPD data by categories within each ecological factor incorporated in our PGLS modeling. **A-E**. Summary statistics of CPD data distribution by ecological factor category. Boxplot: Black line, median; White box, interquartile range; White vertical lines, maximum and minimum. Violin plots: kernel density estimation of data distribution. Wide, high probability; Narrow, low probability. NS, No significant differences among categories; *, $p < 0.008$ (Bonferroni corrected α). Plot colors are to differentiate categories by ecological factor: **A.** Environmental medium, blue colors **B.** Predation strategy, red colors **C**. Environmental light intensity, green colors **D**. Horizontal spatial structure of visual scene, greytones **E.** Eye type, black patterns. App., apposition; N. Sup., neural superposition; Sup., superposition. Note that Eye type was not analyzed in PGLS due to unequal sample sizes.

exemplify each of these factors (Fig. 3). The fact that CPD significantly varies for only two of these four co-factors (environmental medium and foraging strategy) in our uncorrected comparisons (Fig. 2) highlights the importance of correcting for phylogeny when conducting broad species comparisons.

Body size did not correlate with acuity in our phylogenetically-corrected model, despite the linear correlation observed between the log transormation of CPD and body length. The fossil record provides some evidence to support this finding, specifically in relation to foraging strategy. The visual acuities of ancient marine arthropods, Eurypterids and Anomaocarids, are estimated to equate to the acuities of top aquatic arthropod predators alive today (0.35–0.66 CPD; Table 1). Though we cannot be completely certain of the behavioral ecologies of these extinct species, evaluation of the chelicerae feeding appendages and the visual acuity of different Euryptid species suggests a correlation between active predation and high visual acuity (McCoy et al., 2015). Large body size in these extinct animals also does not appear to be consistently associated with increased visual acuity. In particular, the species *Acutiramus cummings* (a non active predator), shows significant decreases in visual acuity with growth, whereby visual acuity is lower in larger specimens (McCoy et al., 2015).

It is possible that, like camera type eyes, compound eye size may be a better allometric predictor of acuity than body size (Caves et al., 2017). The opposing results generated from our phylogenetically-corrected and uncorrected analyses (Fig. S4 and Table 2) provide further evidence for the importance of accounting for phylogenetic distance when conducting meta-analyses of diverse species. Previous studies that found larger body sizes correlated with higher acuities may have been conducted in species whose body sizes scale isometrically with eye size, as was the case

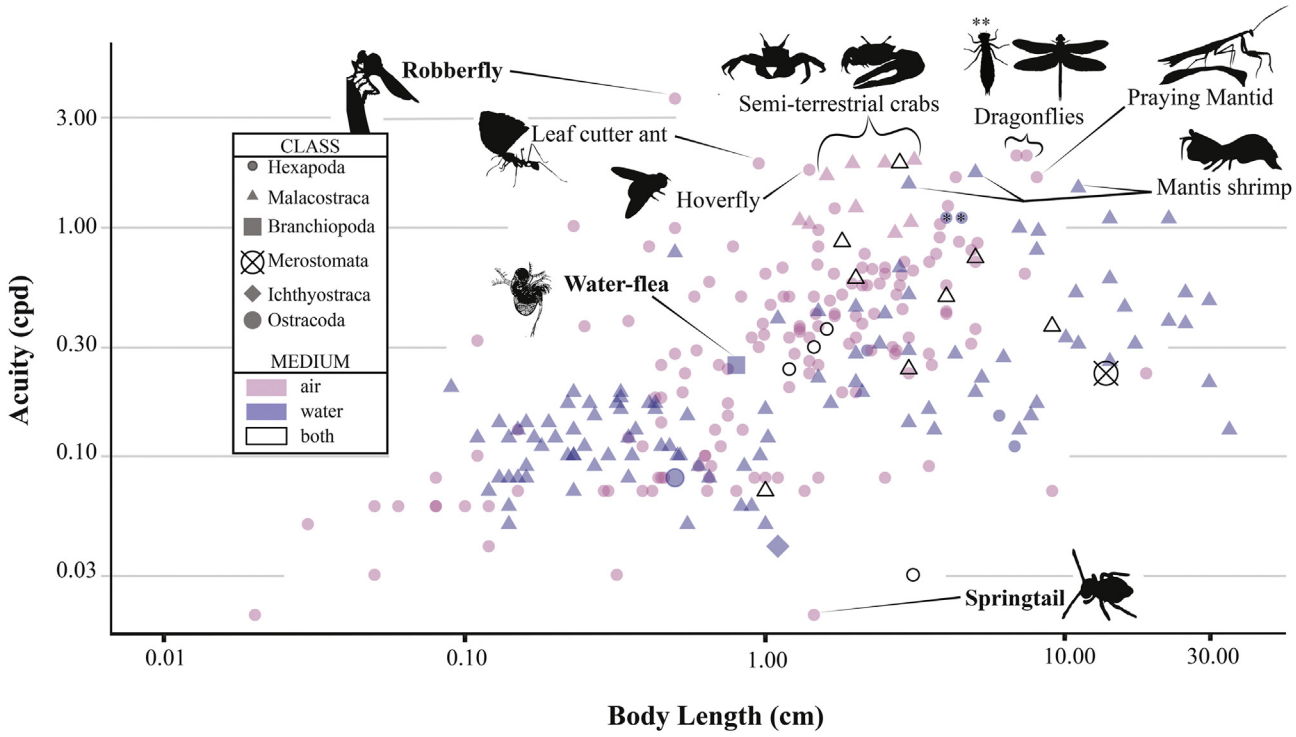

Fig. 3. Plot of body length vs. CPD for the six classes of Arthropoda included in the phylogeny subset data. Arrows, brackets and silhouettes highlight animals with highest visual acuities. ** denote the aquatic larval stages (two blue circles) of the two adult dragonflies in brackets (two red circles). Animals denoted in bold font are represented as possessing the best, worst, and median visual acuities, which are modeled using *AcuityView* software in Fig. 4.

for a study of diurnal bees (Jander and Jander, 2002). We were not able to test how compound eye size correlates with acuity or body size in this study, since eye size is an underreported metric.

There are several additional explanations for why acuity may be poorly linked to body size. Though extremely large eyes (with presumably high visual acuity) are constrained by body size, there is little evolutionary constraint for the reverse. The eyes (or lack thereof) of many cave dwelling species provide a prime example of how evolutionary reductions in eye size leading to loss of acuity can occur independently of changes in body size (Porter and Sumner-Rooney, 2018). Secondly, acute zones of forward facing ommatidia are sometimes, but not always (see Muscidae love spot in Beersma et al., 1977), a common solution for increasing visual acuity without increasing the overall size of the eye, further confounding any potential correlations between body size and acuity. Lastly, body size may only be a limiting factor on eye size and acuity in air where the effects of mass and gravity are more pronounced than they are underwater. A flying insect may thus be constrained in the maximum size of its eye and body, whereas buoyancy may relieve such a constraint in aquatic arthropods. Though aquatic species may not experience the same constraints on the size of their eyes or body, overall, acuity is still much poorer in species that live underwater for reasons evaluated in section 4.3.

4.2. Comparison of compound eye acuities with AcuityView

Our results from inputting the best, worst, and median visual acuity values of our database into *AcuityView* software provide a compelling example of how a visual scene may be perceived at different ecologically relevant distances by viewers with different acuities. For example, the top performer, the robberfly (*H. abdominalis*), maintains an adequate level of resolution even for objects at distance up to 300 cm (Fig. 4C). This is in agreement with studies that have recorded pursuit distances of greater than 53 cm, which is more than 100x the 0.5 cm body length of an individual robberfly (Wardill et al., 2017). Thus, the great range of viewer distances evaluated here likely represent conservative estimates of distance for some species. It is interesting, though perhaps not surprising, to note that the median compound eye visual acuity exemplified by the water-flea (*Polyphemus pediculus*), which is more than 10-times less than the max CPD, corresponds to a 10-fold decrease in the distance at which spatial information remains available. In other words, images viewed by eyes with the median acuity contain spatial detail at 10x the mean body length distance (Fig. 4E), but this information is lost with a 10-fold increase in distance (Fig. 4F). At the other end of the acuity range, the springtail *D. ornata* has very little spatial information available to it even at the closest range, which is approximately two body lengths of this given species (BL = 1.45 cm; Fig. 4G). It is in species with optical resolution in ranges such as this that we might expect visual processing to favor mechanisms of edge enhancement to extract ecologically relevant, spatial information at close range.

4.3. How do multiple ecological factors impact compound eye acuity?

Whether an animal lives in air or water is a fundamental way we describe that animal, yet the extent that these two media influence visual system evolution is relatively understudied outside of amphibious species. This study provides the largest exploration of how environmental medium impacts the evolution of animal vision. As predicted, the highest compound eye visual acuities are all achieved by animals evolved to see in air. In air, vision is an excellent remote detection system. With sufficient acuity, objects and signals can be spotted from a far distance without the viewer being detected. The absorption and scatter of light underwater,

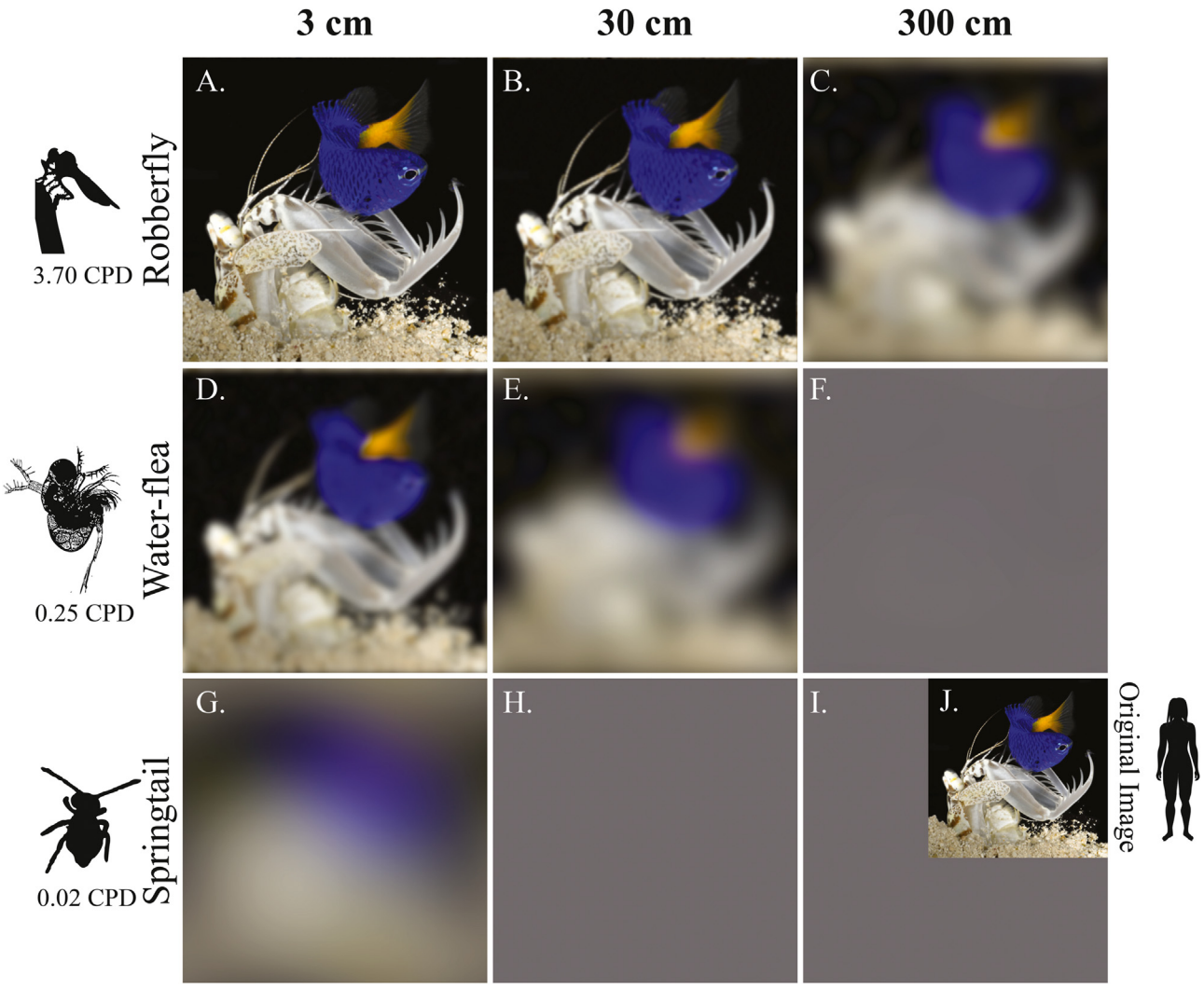

Fig. 4. Simulated differences in the visual perception of a scene based on acuity estimates of three arthropod species. Outputs from the *AcuityView* R package (Caves and Johnsen, 2018) indicate variation in the ability to resolve spatial detail of (A–C) the robberfly (*Holcocephala abdominalis*), (D–F) the springtail (*Dicyrtomina ornata*), and (G–H) the water-flea (*Polyphemus pediculus*) representing the best, median, and worst acuity values listed in our visual acuity database, respectively. Visual perception was modeled over three orders of magnitude relative to the average body length of all species in the database, equaling ~3 cm. Grey squares indicate the total loss of spatial information. Inset panel (J) represents the original image as it would appear to a human observer (60.0 CPD). Photo credit: R.L. Caldwell.

however, reduces the efficacy of vision as a remote sensor by drastically reducing sighting distances (Ruxton and Johnsen, 2016). We see this reflected in our dataset for groups such as mantis shrimp, whose visual acuities are the highest recorded underwater, yet fall well below those achieved for species living in air (Fig. 3).

How does living underwater limit the maximum acuity of a compound eye? The interplay between investment in vision versus other, more salient sensory systems underwater (such as mechanoreception; Popper et al., 2001), may provide an answer to this question. Perhaps, in the aquatic habitat, more reliable remote sensing cues come from multimodal structures (mechano- or chemo-receptors; Nowińska and Brozek, 2020), while vision provides a more proximate cue for detection. This is in line with conclusions drawn from studies of bioluminescent signals in the deep sea that find vision to be insufficient for primary contact between shrimp (Herring, 2000; Schweikert et al., 2020). Studies of predatory visual systems whose life histories evolved across different media (i.e. odonate larvae vs. adults) or who lead amphibious lifestyles (i.e. belostomatids) provide an avenue for testing this hypothesis. The difference in acuity between life stages, in particular, may provide further insight into the ecological co-factors that predict acuity independent of phylogeny. As we can see in the data presented in Fig. 3, aeshnid dragonfly larvae achieve some of the highest visual acuities underwater, yet they are well below the acuities of the adult form. Since both adults and larvae are active hunters, this difference may be the result of inhabiting different media, different modes of movement (flight vs. aquatic), or different environmental light intensity levels narrower than those scored in this study (bright sunlight vs. murky water). Study of additional species that do not switch media over their life history, such as crustaceans, may shed some light on the impact a medium has on visual acuity.

Our second PGLS model found that addition of the horizontal structure of an environmental light field as a co-factor predicts the visual acuity of a compound eye. This result provides an interesting avenue for the application of new methods that characterize the spatial distribution of environmental light fields, such as the Environmental Light Field (ELF) method (Warrant et al., 2020; Nilsson and Smolka, submitted). We know from studies of fish that

scene complexity correlates with acuity (Caves et al., 2017). Horizontal structure is confounded in the definition of a complex visual scene used to evaluate fish acuity, making it difficult to determine whether the horizon is also a key factor in the evolution of camera-type eyes. Scene spatial complexity may only be a factor relevant to an animal with very high visual acuity. The poor resolving power inherent to the median of all compound eyes is unlikely to permit discrimination of a signal or object against a background that may appear complex to a fish at biologically relevant distances (Fig. 4). In this case, the only complexity that may influence an animal wielding such compound eyes is the horizontal structure of a scene coupled to a substrate. It is important to consider the possibility that different selective forces may act on vertebrate and invertebrate systems. Caution should, therefore, be exercised when comparing the drivers of visual acuity evolution among taxa with compound versus camera-type eyes.

No significant differences were observed among the three categories of eye type. There is a trend, however, in neural superposition eyes, towards greater acuities than apposition or superposition eye types. Since neural superposition eye types are only represented in one lineage in our dataset, dipteran flies, this may be the result of co-factors selecting for higher acuity, such as variable lighting conditions and active predation strategies in certain species, rather than an inherent property of the eye type itself. Alternatively, evolution of the neural superposition eye type may have derived from selection towards a need for more acute vision itself.

Additionally, acuity did not significantly differ between apposition and superposition optics, despite their wide distribution among arthropods (Land, 1997; Cronin and Porter, 2008). We expected to see lower acuities associated with superposition optics given that spatial pooling is inherent to this eye type, though we did not. This result may be related to neural tuning mechanisms that allow for flexibility between resolution and sensitivity (i.e. Stöckl et al., 2020) and thus producing higher acuities in some superposition eyes (Land, 1984). Alternatively, superposition eye acuity may seem higher than expected due to a lack in reporting of the true acceptance angles of photoreceptors in superposition eyes. Interommatidial angle is the most common metric reported for a compound visual system, which is reflected by over half of the entries in our database. Only 81 of the total entries in the database are direct reports of acceptance angle, 14 of which are from superposition eyes. In a superposition eye, multiple optical features may lead to larger acceptance angles than one would predict from the interommatidial angle alone (i.e. the owlfly *Libelloides macaronius*, Belusic et al., 2013). Thus, acuity may be overestimated when only interommatidial angle information is available. Given acuity is a labile trait under the influence of multiple pressures, it is also possible that eye type is simply not as strong a predictor of visual acuity as medium, foraging strategy, and environmental light intensity.

4.4. Concluding remarks

In summary, this study accomplishes three major goals. First, we present Table 1 and the corresponding phylogeny as new resources for researchers working on the ecology and evolution of arthropod visual systems. By including other factors of interest, researchers may be able to build from our database to test additional questions related to the evolution of complex traits, visual or otherwise. Our database is also an excellent resource for researchers seeking to design appropriate visual stimuli for a given system. For example, when designing behavioral assays, it is important to note the visual acuity of an animal to ensure a given stimulus is detectable or resolvable by that species' visual system.

Second, we provide evidence that multiple ecological factors influence the evolution of visual acuity. Though environmental light intensity is universally accepted as a driver of visual evolution, this study found that additional factors (such as environmental medium and predation strategy) may hold more or additional weight in shaping acuity. These results provide an excellent starting point for experiments that seek to test the role of acuity in arthropod ecology, particularly in the underwater environment. For instance, how does acuity vary among animals that occupy different underwater conditions, environments with restricted environmental spectra and contrast, or across more finely categorized (and quantified) ranges of light intensities?

Finally, we provide evidence for two new avenues of investigation into previously untested factors that affect compound eye acuity: environmental medium and horizontal structure of the visual scene. These two factors open the door to future studies that consider visual evolution in the context of multimodal sensing, as well as ways to incorporate new methods for characterizing the external world. Overall, this study presents additional evidence to support the need for more comparative experiments that consider the effects of phylogenetic relationship when evaluating the impact of ecological factors on organismal traits. In this way we can more accurately study the universal forces and principles that drive the evolution of animal vision.

Author Statement

Kathryn Feller: Conceptualization, Methodology, Formal Analysis, Investigation, Data Curation, Software, Writing – Original Draft, Writing – Review and Editing, Visualization, Supervision, Project Administration. **Camilla Sharkey:** Methodology, Formal Analysis, Investigation, Data Curation, Software, Writing – Original Draft, Writing – Review and Editing, Visualization. **Alyssa McDuffee-Altekruse:** Investigation, Data Curation, Writing – Original Draft, Writing – Review and Editing. **Heather Bracken-Grissom:** Validation, Investigation, Writing – Original Draft, Writing – Review and Editing. **Nathan Lord:** Validation, Investigation, Writing – Original Draft, Writing – Review and Editing, Visualization. **Megan Porter:** Validation, Investigation, Writing – Original Draft, Writing – Review and Editing. **Lorian Schweikert:** Methodology, Formal Analysis, Investigation, Data Curation, Software, Writing – Original Draft, Writing – Review and Editing, Visualization.

Acknowledgements

Thank you to Eleanor Caves and Laura Bagge for their feedback as well as input from our anonymous reviewers, whose insightful comments and suggestions elevated the quality of this manuscript. Thank you to Roy Caldwell for sharing his compelling photograph of invertebrate predation upon a vertebrate. Thank you also to Anton Suvorov for his phylogeny advice and insight. Also, a tremendous thank you to the many researchers who generated the data upon which this study is based. This work is contribution #222 from the Coastlines and Oceans Division of the Institute of Environment at Florida International University.

Appendix A. Supplementary data

Supplementary data to this article can be found online at https://doi.org/10.1016/j.asd.2020.101002.

Funding

No specific funding source was associated with this work.

Contributions

Original idea, design and orchestration of research team by KDF. Database was assembled by KDF, LES, CRS, and AMA. Phylogeny constructed by CRS with input from HBG, NPL, and MLP. PGLS design and execution by LES and KDF. Ecological factor scoring by KDF and LES, with review and approval by HBG, NPL, and MLP. CRS and NPL constructed phylogenetic figures. All remaining figures and text composed by KDF, with contributions and edits from all authors.

References

Abadi, S., Azouri, D., Pupko, T., Mayrose, I., 2019. Model selection may not be a mandatory step for phylogeny reconstruction. Nat. Commun. 10, 934.
Adams, D.C., 2008. Phylogenetic meta-analysis. Evolution 62, 567–572.
Anisimova, M., Gil, M., Dufayard, J.F., Dessimoz, C., Gascuel, O., 2011. Survey of branch support methods demonstrates accuracy, power, and robustness of fast likelihood-based approximation schemes. Syst. Biol. 60, 685–699.
Belusic, G., Pirih, P., Stavenga, D.G., 2013. A cute and highly contrast-sensitive superposition eye - the diurnal owlfly *Libelloides macaronius*. J. Exp. Biol. 216, 2081–2088.
Beersma, D.G.M., Stavenga, D.G., Kuiper, J.W., 1977. Retinal lattice, visual field and binocularities in flies. J. Comp. Physiol. 119 (3), 207–220.
Budelmann, B.U., 1989. Hydrodynamic receptor systems in invertebrates. In: Coombs, S. (Ed.), The Mechanosensory Lateral Line. New York, pp. 607–631.
Burnham, K.P., Anderson, D.R., 2002. Multimodel inference: understanding AIC and BIC in model selection. Socio. Methods Res. 33, 261–304.
Burnham, K.P., Anderson, D.R., Huyvaert, K.P., 2011. AIC model selection and multimodel inference in behavioral ecology: some background, observations, and comparisons. Behav. Ecol. Sociobiol. 65, 23–35.
Bybee, S.M., Bracken-Grissom, H., Haynes, B.D., Hermansen, R.A., Byers, R.L., Clement, M.J., Udall, J.A., Wilcox, E.R., Crandall, K.A., 2011. Targeted amplicon sequencing (TAS): a scalable next-gen approach to multilocus, multitaxa phylogenetics. Genome Biol. Evol. 3, 1312–1323.
Capella-Gutiérrez, S., Silla-Martínez, J.M., Gabaldón, T., 2009. trimAl: a tool for automated alignment trimming in large-scale phylogenetic analyses. Bioinformatics 25, 1972–1973.
Caves, E.M., Johnsen, S., 2018. AcuityView: an r package for portraying the effects of visual acuity on scenes observed by an animal. Methods Ecol. Evol. 9 (3), 793–797.
Caves, E.M., Brandley, N.C., Johnsen, S., 2018. Visual acuity and the evolution of signals. Trends Ecol. Evol. 1–15.
Caves, E.M., Frank, T.M., Johnsen, S., 2016. Spectral sensitivity, spatial resolution and temporal resolution and their implications for conspecific signalling in cleaner shrimp. J. Exp. Biol. 219, 597–608.
Caves, E.M., Sutton, T.T., Johnsen, S., 2017. Visual acuity in ray-finned fishes correlates with eye size and habitat. J. Exp. Biol. 220, 1586–1596.
Cronin, T.W., 1986. Optical design and evolutionary adaptation in crustacean compound eyes. J. Crustac Biol. 6, 1–24.
Cronin, T.W., Johnsen, S.J., Marshall, J.N., Warrant, E.J., 2014. Visual Ecology. Princeton University Press.
Cronin, T.W., Porter, M.L., 2008. Exceptional variation on a common theme: the evolution of Crustacean compound eyes. Evolution: Educ. Outreach 1, 463–475.
Farnier, K., Dyer, A.G., Taylor, G.S., Peters, R.A., Steinbauer, M.J., 2015. Visual acuity trade-offs and microhabitat-driven adaptation of searching behaviour in psyllids (Hemiptera: Psylloidea: Aphalaridae). J. Exp. Biol. 218, 2660.
Freckleton, R.P., Harvey, P.H., Pagel, M., 2002. Phylogenetic analysis and comparative data: a test and review of evidence. Am. Nat. 160, 712–726.
Gaspar, P., Arif, S., Sumner-Rooney, L., Kittelmann, M., Bodey, A.J., Stern, D.L., Nunes, M.D.S., McGregor, A.P., 2020. Characterization of the genetic architecture underlying eye size variation within *Drosophila melanogaster* and *Drosophila simulans*. G GenesGenomesGenetics 10, 1005–1018.
Gonzalez-Bellido, P.T., Wardill, T.J., Juusola, M., 2011. Compound eyes and retinal information processing in miniature dipteran species match their specific ecological demands. Proc. Natl. Acad. Sci. Unit. States Am. 108, 4224–4229.
Gould, S.J., Lewontin, R.C., 1979. The spandrels of San Marco and the Panglossian paradigm: a critique of the adaptationist programme. Proc. Roy. Soc. Lond. B Biol. Sci. 205, 581–598.
Herring, P., 2000. Species abundance, sexual encounter and bioluminescent signalling in the deep sea. Phil. Trans. Roy. Soc. Lond. B Biol. Sci. 355, 1273–1276.
Hoang, D.T., Chernomor, O., von Haeseler, A., Minh, B.Q., Vinh, L.S., 2018. UFBoot2: improving the ultrafast bootstrap approximation. Mol. Biol. Evol. 35, 518–522.
Horká, I., De Grave, S., Fransen, C.H.J.M., Petrusek, A., Ďuriš, Z., 2016. Multiple host switching events shape the evolution of symbiotic palaemonid shrimps (Crustacea: Decapoda), 6. Nature Publishing Group, p. 26486.
Jander, U., Jander, R., 2002. Allometry and resolution of bee eyes (Apoidea). Arthropod Struct. Dev. 30, 179–193.
Jerlov, N.G., 1977. Classification of sea water in terms of quanta irradiance. ICES (Int. Counc. Explor. Sea) J. Mar. Sci. 37, 281–287.
Johnsen, S., 2002. Cryptic and conspicuous coloration in the pelagic environment. Proc. Roy. Soc. Lond. B Biol. Sci. 269, 243–256.
Johnsen, S., 2012. The Optics of Life: a Biologist's Guide to Light in Nature. Princeton University Press.
Kalyaanamoorthy, S., Minh, B.Q., Wong, T.K.F., von Haeseler, A., Jermiin, L.S., 2017. ModelFinder: fast model selection for accurate phylogenetic estimates. Nat. Methods 14, 587–589.
Katoh, K., Misawa, K., Kuma, K., Miyata, T., 2002. MAFFT: a novel method for rapid multiple sequence alignment based on fast Fourier transform. Nucleic Acids Res. 30, 3059–3066.
Katoh, K., Standley, D.M., 2013. MAFFT multiple sequence alignment software version 7: improvements in performance and usability. Mol. Biol. Evol. 30, 772–780.
Kawahara, A.Y., Plotkin, D., Espeland, M., Meusemann, K., Toussaint, E.F.A., Donath, A., Gimnich, F., Frandsen, P.B., Zwick, A., dos Reis, M., Barber, J.R., Peters, R.S., Liu, S., Zhou, X., Mayer, C., Podsiadlowski, L., Storer, C., Yack, J.E., Misof, B., Breinholt, J.W., 2019. Phylogenomics reveals the evolutionary timing and pattern of butterflies and moths. Proc. Natl. Acad. Sci. Unit. States Am. 116, 22657–22663.
Kirschfeld, K., 1976. The resolution of lens and compound eyes. In: Neural Principles in Vision. Berlin, pp. 354–370.
Land, M.F., 1984. The resolving power of diurnal superposition eyes measured with an ophthalmoscope. J. Comp. Physiol. 154, 515–533.
Land, M.F., 1997. Visual acuity in insects. Annu. Rev. Entomol. 42, 147–177.
Land, M.F., Nilsson, D.-E., 2002. Animal Eyes. Oxford University Press, Oxford.
Lozano-Fernandez, J., Giacomelli, M., Fleming, J.F., Chen, A., Vinther, J., Thomsen, P.F., Glenner, H., Palero, F., Legg, D.A., Iliffe, T.M., Pisani, D., Olesen, J., 2019. Pancrustacean evolution illuminated by taxon-rich genomic-scale data sets with an expanded remipede sampling. Genome Biol. Evol. 11, 2055–2070.
McCoy, V.E., Lamsdell, J.C., Poschmann, M., Anderson, R.P., Briggs, D.E., 2015. All the better to see you with: eyes and claws reveal the evolution of divergent ecological roles in giant pterygotid eurypterids. Biol. Lett. 11, 20150564.
Misof, B., Liu, S., Meusemann, K., Peters, R.S., Donath, A., Mayer, C., Frandsen, P.B., Ware, J., Flouri, T., Beutel, R.G., Niehuis, O., 2014. Phylogenomics resolves the timing and pattern of insect evolution. Science 346, 763–767.
Nguyen, L.-T., Schmidt, H.A., von Haeseler, A., Minh, B.Q., 2015. IQ-TREE: a fast and effective stochastic algorithm for estimating maximum-likelihood phylogenies. Mol. Biol. Evol. 32, 268–274.
Nilsson, D.-E., Smolka, J., Quantifying Biologically Essential Aspects of Environmental Light. (submitted). Lund University.
Nowińska, A., Brozek, J., 2020. Insect evolution toward aquatic habitats; reassessment of antennal sensilla in the water bug families Ochteridae, Gelastocoridae and Aphelocheiridae (Hemiptera: heteroptera: Nepomorpha). Contrib. Zool. 1–22.
Osorio, D., Vorobyev, M., 1996. Colour vision as an adaptation to frugivory in primates. Proc. R. Soc. Lond. B Biol. Sci. 263, 593–599.
Pagel, M., 1999. Inferring the historical patterns of biological evolution. Nature 401, 877–884.
Popper, A.N., Salmon, M., Horch, K.W., 2001. Acoustic detection and communication by decapod crustaceans. J. Comp. Physiol.: Neuroethol. Sensory Neural Behav. Physiol. 187, 83–89.
Porter, M.L., 2005. Crustacean Phylogenetic Systematics and Opsin Evolution. Thesis Brigham Young University, Provo UT.
Porter, M.L., Sumner-Rooney, L., 2018. Evolution in the dark: unifying our understanding of eye loss. Integr. Comp. Biol. 58, 367–371.
Porter, M.L., Zhang, Y., Desai, S., Caldwell, R., Cronin, T., 2010. Evolution of Anatomical and Physiological Specialization in the Compound Eyes of Stomatopod Crustaceans, 213, pp. 3473–3486.
Revell, L.J., 2011. phytools: an R package for phylogenetic comparative biology (and other things). Methods Ecol. Evol. 3, 217–223.
Rutowski, R.L., Gislén, L., Warrant, E.J., 2009. Visual acuity and sensitivity increase allometrically with body size in butterflies. Arthropod Struct. Dev. 38, 91–100.
Ruxton, G.D., Johnsen, S., 2016. The effect of aggregation on visibility in open water. Proc. R. Soc. Lond. B Biol. Sci. 283, 20161463–20161467.
Scales, J.A., Butler, M.A., 2016. The relationship between microhabitat use, allometry and functional variation in the eyes of Hawaiian Megalagrion damselflies. Funct. Ecol. 30, 356–368.
Schindelin, J., Arganda-Carreras, I., Frise, E., Kaynig, V., Longair, M., Pietzsch, T., Preibisch, S., Rueden, C., Saalfeld, S., Schmid, B., Tinevez, J.-Y., White, D.J., Hartenstein, V., Eliceiri, K., Tomancak, P., Cardona, A., 2012. Fiji: an open-source platform for biological-image analysis. Nat. Methods 9, 676–682.
Schweikert, L.E., Caves, E.M., Solie, S.E., Sutton, T.T., Johnsen, S., 2018. Variation in rod spectral sensitivity of fishes is best predicted by habitat and depth. J. Fish. Biol. 95, 179–185.
Schweikert, L.E., Davis, A.L., Johnsen, S., Bracken-Grissom, H.D., 2020. Visual perception of light organ patterns in deep-sea shrimps and implications for conspecific recognition. Ecol. Evol. 10, 9503–9513.
Schwentner, M., Combosch, D.J., Pakes Nelson, J., Giribet, G., 2017. A Phylogenomic Solution to the origin of insects by resolving crustacean-hexapod relationships. Curr. Biol. 27, 1818–1824.
Sharkey, C.R., Partridge, J.C., Roberts, N.W., 2015. Polarization sensitivity as a visual contrast enhancer in the Emperor dragonfly larva, *Anax imperator*. J. Exp. Biol. 218, 3399–3405.

Smolka, J., Hemmi, J.M., 2009. Topography of vision and behaviour. J. Exp. Biol. 212, 3522–3532.
Stöckl, A.L., O'Carroll, D.C., Warrant, E.J., 2020. Hawkmoth lamina monopolar cells act as dynamic spatial filters to optimize vision at different light levels. Sci. Adv. 6, 1–8.
Tung Ho, L. si, Ané, C., 2014. A linear-time algorithm for Gaussian and non-Gaussian trait evolution models. Syst. Biol. 63, 397–408.
Vaidya, G., Lohman, D.J., Meier, R., 2011. SequenceMatrix: concatenation software for the fast assembly of multi-gene datasets with character set and codon information. Cladistics 27, 171–180.
Van Der Wal, C., Ahyong, S.T., Ho, S.Y.W., Lo, N., 2017. The evolutionary history of Stomatopoda (Crustacea: Malacostraca) inferred from molecular data. PeerJ 5 e3844–17.
Veilleux, C.C., Kirk, E.C., 2014. Visual acuity in mammals: effects of eye size and ecology. Brain Behav. Evol. 83, 43–53.
von Reumont, B.M., Jenner, R.A., Wills, M.A., Dell'ampio, E., Pass, G., Ebersberger, I., Meyer, B., Koenemann, S., Iliffe, T.M., Stamatakis, A., Niehuis, O., Meusemann, K., Misof, B., 2012. Pancrustacean phylogeny in the light of new phylogenomic data: support for Remipedia as the possible sister group of Hexapoda. Mol. Biol. Evol. 29, 1031–1045.
Wardill, T.J., Fabian, S.T., Pettigrew, A.C., Stavenga, D.G., Nordström, K., Gonzalez-Bellido, P.T., 2017. A novel interception strategy in a miniature robber fly with extreme visual acuity. Curr. Biol. 27, 854–859.
Warrant, E., 2008. Seeing in the dark: vision and visual behaviour in nocturnal bees and wasps. J. Exp. Biol. 211, 1737.
Warrant, E., Johnsen, S., Nilsson, D.-E., 2020. Light and visual environments. In: The Senses: A Comprehensive Reference, second ed., pp. 1–26.
Warrant, E., Porombka, T., Kirchner, W.H., 1996. Neural image enhancement allows honeybees to see at night. Proc. Roy. Soc. Lond. B 263, 1521–1526.
Warrant, E.J., McIntyre, P.D., 1993. Arthropod eye design and the physical limits to spatial resolving power. Prog. Neurobiol. 40, 413–461.
Zeil, J., Hemmi, J.M., 2005. The visual ecology of fiddler crabs. J. Comp. Physiol.: Neuroethol. Sensory Neural Behav. Physiol. 192, 1–25.